Decision Science Letters 13 (2024) 921–950

Contents lists available at GrowingScience

Decision Science Letters

homepage: www.GrowingScience.com/dsl

A novel multi-objective stochastic model and a novel hybrid metaheuristic for designing supply chain network under disruption risks to enhance supply chain resilience

Mohammad Mahdi Vali-Siar[a*], Hanieh Shekarabi[b] and Emad Roghanian[c]

[a]*School of Industrial Engineering, Iran University of Science and Technology, Tehran, Iran*
[b]*Department of Industrial Engineering, Faculty of Engineering, Kharazmi University, Tehran, Iran*
[c]*Department of Industrial Engineering, K. N. Toosi University of Technology, Tehran, Iran*

C H R O N I C L E

Article history:
Received: February 20, 2024
Received in the revised format: June 21, 2024
Accepted: July 30, 2024
Available online: July 30, 2024

Keywords:
Supply chain network design
Disruption risks
Resilience
Metaheuristics
Environmental sustainability

A B S T R A C T

Supply chains are vulnerable to various disruption risks that can adversely affect their overall performance and objectives. This study addresses the challenge of designing a resilient and environmentally sustainable mixed open and closed-loop supply chain network that can withstand both operational and disruption risks. The research employs a bi-objective stochastic mathematical model to examine the balance between environmental sustainability and profitability within the SC. To mitigate the impact of disruptions, several resilience strategies are incorporated into the model, significantly reducing their adverse effects. Due to the inherent complexity of the problem, the study introduces a novel hybrid metaheuristic algorithm that combines ant colony optimization with teaching and learning-based optimization, named ACO-TLBO. Additionally, two other enhanced hybrid metaheuristics are proposed. The performance of these solution methods is assessed through various test problems, using specific performance metrics for comparison. Results reveal that the ACO-TLBO algorithm excels in generating high-quality, non-dominated solutions. The model's practical applicability is demonstrated through a case study in the tire industry, validating its effectiveness. The findings indicate that the proposed resilience strategies are crucial for minimizing the negative impacts of disruptions on SC objectives. Furthermore, the results underscore the importance of resilience in maintaining both sustainability and profitability within supply chains.

1. Introduction

Modern organizations aim to leverage effective supply chain management (SCM) to improve their market position, gain competitive advantages, reduce costs, and enhance overall supply chain (SC) efficiency. Among the critical aspects of SCM is supply chain network design (SCND), which involves making strategic decisions that shape the physical structure of the SC. SCND encompasses decisions related to the location, number, and capacity of facilities, as well as the selection of suppliers, among other considerations. These decisions are pivotal in optimizing the SC's performance and ensuring its operational success (Govindan et al., 2017). One of the most severe challenges facing humanity today is climate change (Meng et al., 2020). The rapid increase in the global population has driven a surge in energy consumption to meet the rising demands, thereby accelerating climate change and global warming (Ramezanian et al., 2019). These challenges, compounded by the depletion and rising use of non-renewable resources, environmental pollution, and the enactment of environmental regulations in many countries, have prompted researchers and industry leaders to focus on the implementation of reverse logistics (Soleimani et al., 2017). By developing reverse and closed/open-loop SCs, sustainability can be significantly enhanced, as these approaches are highly effective in reducing energy and material consumption as well as environmental pollution.

* Corresponding author.
E-mail address: mvalisiar@gmail.com (M. M. Vali-Siar)

doi: 10.5267/dsl.2024.7.005

Supply chain network (SCN) structures are generally categorized into three types: forward, reverse, and networks that incorporate both reverse and forward flows. This third category is further divided into three subtypes: open-loop, closed-loop, and a combination of both, known as mixed open and closed-loop structures (Van Engeland et al., 2020). In mixed SCs, some recycled materials and products are retained and reused within the SC, while the remainder exits the SC and enters other SCs for similar or different applications (Salema et al., 2007). SCs are vulnerable to various risks, which can be broadly classified into operational risks and disruption risks. Operational risks arise from the inherent uncertainties within SCs, such as fluctuations in supply, variations in lead times, changes in shipping durations, and cost variability. On the other hand, disruption risks stem from potential interruptions that can affect any segment of the SC, caused by natural disasters, human-related threats, or technical failures (Sabouhi et al., 2018). These disruptions significantly impact and negatively influence the goals and performance of the SC (Torabi et al., 2016). New SCs are particularly susceptible to disruptions due to their amplified length and intricate structure (Namdar et al., 2018). Among the notable disruptions in recent history, the COVID-19 pandemic has emerged as a global upheaval with far-reaching ramifications, profoundly impacting SCs across the globe. This unprecedented crisis has precipitated a downturn in SC performance, marked by logistical setbacks such as delayed deliveries, scarcity of essential raw materials, and upheavals in transportation networks attributable to pandemic-related constraints. It has precipitated a downturn in SC performance, marked by logistical setbacks such as delayed deliveries, scarcity of essential raw materials, and upheavals in transportation networks attributable to pandemic-related constraints (Karmaker et al., 2021). Consequently, the resilience of SCs—their capacity to withstand, adapt to, and rebound from disruptions while preserving or attaining a revised operational equilibrium—has come under escalating scrutiny (Ivanov & Dolgui, 2020), which is the capability of the SC to cope with and adapt to disruptions and restore to pre-disruption or a new desired state to respond to demand and maintain proper performance (Hosseini et al., 2019). The design of an SC exerts a pivotal influence on its resilience, with firms endowed with well-structured SCs demonstrating heightened resilience in the face of disruptions (Klibi et al., 2010). The integration of sustainability and resilience is imperative for ensuring the longevity of systems, leveraging the synergistic potential inherent in these concepts Concurrently, the resilience of a SC is paramount for sustaining its optimal performance in terms of sustainability (Mehrjerdi & Shafiee, 2021).

This study investigates the design and redesign of a green mixed SC network under disruptive conditions, introducing a novel bi-objective mathematical model aimed at maximizing total profitability while minimizing adverse environmental impacts. To enhance the network's resilience and mitigate disruptions, various resilience strategies are implemented. The complexity of the problem is addressed through the proposition of three hybrid metaheuristics. Additionally, empirical validation of the mathematical model and solution methodologies is provided through a real-life case study and diverse numerical instances, demonstrating the practicality of the examined problem and facilitating comprehensive analysis.
The paper is structured as follows: Section 2 conducts a comprehensive review of pertinent literature. Section 3 delineates the problem statement and outlines the proposed optimization model. Solution methodologies are expounded upon in Section 4. Section 5 furnishes details of the case study, test scenarios, computational findings, and subsequent analyses. Finally, Section 6 offers concluding remarks.

2. Literature review

Within this section, an examination of literature pertaining to resilient SCND, green SCND, and the intersection of resilient and green SCND is presented succinctly. Following a comprehensive review of prior scholarship, the final subsection identifies research lacunae and elucidates the contributions of the present study.

2.1 Green supply chain network design

In light of the extensive literature on green SCND, this section undertakes a focused review of papers directly relevant to our research. Specifically, attention is directed toward studies examining green SC design while incorporating considerations of reverse logistics. Zohal & Soleimani (2016) investigated a green closed-loop SCND problem within the gold industry, presenting a multi-objective mixed integer linear programming (MILP) model. Their model aimed to minimize costs, maximize income, and reduce CO2 emissions. Nurjanni et al. (2017) formulated a bi-objective mathematical model for the green closed-loop SCND problem, with objectives centered on cost minimization and environmental impact reduction. (Mohtashami et al., 2020) utilized queuing system concepts to design closed-loop SC systems, targeting the minimization of negative environmental impacts and energy consumption. Similar endeavors in the literature include the works of Rad & Nahavandi (2018) and Mardan et al. (2019). However, these aforementioned studies did not address uncertainty within their problem formulations, Some researchers have explored the implications of uncertainty on closed-loop green SCND. Soleimani et al. (2017) proposed a tri-objective optimization model for green SCND under uncertainties in demands and social impacts, aiming to simultaneously maximize profit, meet demand satisfaction, and minimize lost workdays. Ghomi-Avili et al. (2018) investigated competitive green closed-loop SCND amidst disruptions faced by suppliers, devising a bi-objective mathematical model focused on maximizing SC profit and minimizing CO2 emissions. Further investigations into green closed-loop SCND under uncertainty have been conducted by Zhen et al. (2019) and Boronoos et al. (2021). Moreover, Valizadeh et al. (2024) presented a new method for managing sustainability risks in closed-loop SCs using a hybrid optimization model. In this study, a bi-level mathematical model was proposed, addressing government concerns at the upper level and manufacturers' decisions at the lower level. Dehshiri & Amiri (2024) integrated Circular Economy principles into SCs. This integration seeks to improve sustainable competitive advantage by developing Closed-Loop SCND and establishing a circular SC that meets economic, environmental, and social objectives. Furthermore, some studies have embarked on green SCN redesign (Feitó-Cespón et al., 2021; Feitó-Cespón et al., 2017; Shahparvari et al., 2021; Yousefi-Babadi et al., 2023).

2.2 Resilient supply chain network design

The field of resilient SCND is experiencing significant growth, particularly underscored by the heightened awareness of its importance in light of the COVID-19 pandemic. Within the realm of resilient SCND, a predominant focus lies on the deployment of resilience strategies to address disruptions. Multiple sourcing emerges as a prominent strategy, embraced by several researchers such as Peng et al. (2011), Hasani & Khosrojerdi (2016), Rezapour et al. (2017), Sabouhi et al. (2018), Bottani et al. (2019), Sabouhi et al. (2020) and Gholami-Zanjani et al. (2021).This approach entails enabling downstream facilities to be served by multiple upstream facilities, thereby mitigating operational interruptions and minimizing damages in the event of upstream facility failures. Facility fortification represents another resilience strategy, wherein facilities are fortified against disruptions at various levels (Fattahi et al., 2017). This fortification enhances facility resilience, albeit with an associated increase in costs, as demonstrated by various studies including Azad et al. (2013), Jabbarzadeh et al. (2016), Fattahi et al. (2017), and Gholami-Zanjani et al. (2021). The utilization of backup facilities serves as an additional resilience strategy, ensuring continuity of operations by substituting failed facilities with backups used in some papers such as Sadghiani et al. (2015), Jabbarzadeh et al. (2016), Sabouhi et al. (2020), and Gholami-Zanjani et al. (2021). Capacity expansion strategies are deployed to augment facility capacities in the face of disruptions. This strategy has been implemented in some studies such as Sabouhi et al. (2020), Gholami-Zanjani et al. (2021), and Shekarabi et al. (2024).
Lateral transshipment strategies facilitate the transfer of products and materials between facilities within the same echelon, thereby enabling efficient resource allocation during disruptions. Jabbarzadeh, Haughton, & Khosrojerdi (2018), and Sabouhi et al. (2020) have both employed this strategy in their studies. Keeping inventory emerges as a fundamental resilience strategy, safeguarding against material and product shortages during disruptions. This strategy has been implemented in studies conducted by Hasani & Khosrojerdi (2016), as well as Sabouhi et al. (2018) exemplify its application in scholarly research.

Additional strategies, such as an alternative bill of material adaptation (Hasani & Khosrojerdi, 2016) and dual-channel distribution (Sabouhi et al., 2020), may prove beneficial depending on the specific structure of the problem at hand. In terms of network structure, the majority of research has traditionally focused on the design of forward SCs. However, some studies have delved into resilient closed-loop SCND under disruption risks, employing stochastic robust optimization models to address the inherent uncertainties (Arabi & Gholamian, 2023; Jabbarzadeh, Haughton, & Khosrojerdi, 2018). Additionally, certain researchers have broadened the scope of their SCND problems by considering concepts beyond resilience. For instance, some have investigated resilient and responsive SCND problems. (Fattahi et al., 2017; Ribeiro & Barbosa-Póvoa, 2023; Sabouhi et al., 2020), while others have examined competition within resilient SCND problems under disruptions (Ghavamifar et al., 2018; Li & Zhang, 2024; Rezapour et al., 2017). Besides, some studies have delved into definition of resilience criteria Such as robustness, agility, leanness, flexibility, and integrality (Rezaei & Liu, 2024). In terms of resilient SCN redesign, some studies have explored mixed SC redesign amidst operational and disruption risks (Vali-Siar & Roghanian, 2020). Others have investigated SCN redesign to address parameter uncertainty and system disruptions (Yousefi-Babadi et al., 2022). Moreover, the integration of environmental concerns into resilient SCND, often referred to as green and resilient SCND, has emerged as a critical area of inquiry, as elucidated in subsequent subsections.

2.3 Green and resilient supply chain network design

Given the paramount significance of incorporating environmental considerations and addressing disruptions' impact on SC objectives, such as environmental goals, the concurrent consideration of resilience and environmental concerns emerges as a pivotal endeavor. The realm of green and resilient SCND appears to be a burgeoning area of scholarly inquiry, with several pertinent issues yet to be thoroughly investigated, particularly concerning SC designs integrating reverse logistics. (Fahimnia et al., 2018) adopted an environmental performance evaluation approach coupled with a robustness measure to tackle environmental concerns and resilience within the SCND paradigm, proposing a single-objective mathematical model. Mohammed et al. (2019) delved into the green and resilient SCND problem, formulating a tri-objective mathematical model aimed at minimizing total costs, CO2 emissions, and maximizing SC resilience. Some researchers utilized resilience strategies to mitigate disruptions Several researchers have leveraged resilience strategies to mitigate disruptions. Hasani et al. (2021) used facility fortification, facility dispersion, semi-finished goods production, and multiple sourcing strategies for designing a resilient and green SCND employed a combination of facility fortification, dispersion, semi-finished goods production, and multiple sourcing strategies to devise a resilient and green SCND framework. Gholami-Zanjani et al. (2021) incorporated multiple sourcing and backup supplier strategies in the design of green and resilient meat SCN.
However, the aforementioned studies overlooked the integration of reverse logistics, Yavari & Zaker (2019) proposed a bi-objective MILP model for resilient and green closed-loop SCND within the dairy industry, introducing an interdependent two-layer structure to account for disruptions in the electric power network supplying the SC's power. Their model aimed

to minimize SC costs and carbon emissions. Moreover, Saeed et al. (2024) integrated green SC practices and resilience strategies within a closed-loop SC through a three-phase methodology. They first develop a MILP model to enhance resilience while minimizing greenhouse gas emissions and costs. Next, they introduce a four-valued neutrosophic optimization algorithm that incorporates truth, falsity, contradictions, and uncertainty. Finally, they apply their model to a smartphone SC case study, promoting circular economy practices. Another category of research has explored sustainability and resilience within the SCND context. Jabbarzadeh, Fahimnia, & Sabouhi (2018), Mehrjerdi & Shafiee (2021), Sazvar et al. (2021), Sabouhi et al. (2021), Fazli-Khalaf et al. (2021), Vali-Siar & Roghanian (2022), Abbasian et al. (2023), and Sharma et al. (2023) have investigated the sustainable and resilient SCND problem from various perspectives. Additionally, Nikian et al. (2023) have focused on enhancing green closed-loop SC resilience in the face of sever disasters and pandemics through robust optimization and multi-objective mathematical models for SCN redesign.

2.4 Research Gaps

Table 1 provides a summary of relevant papers along with their key characteristics. The analysis reveals a notable gap in the literature concerning SCND problems that jointly consider resilience and environmental concerns within networks incorporating reverse logistics (closed-loop, open-loop, and mixed configurations). Remarkably, only one paper addresses this issue, focusing exclusively on closed-loop network structures. Furthermore, the simultaneous integration of resilience, environmental sustainability, and responsiveness has not been explored in prior studies. Merely three papers have investigated responsive and resilient SCND, indicating the need for further exploration in this domain. Resilient mixed SCND has also been overlooked, with exceptions found in the works of Vali-Siar & Roghanian (2020) and Vali-Siar & Roghanian (2022). Notably, a few papers have discussed resilient SCN redesign, highlighting another research gap in this area. Upon scrutiny of Table 1, it becomes evident that the optimization model developed in this paper is more comprehensive compared to previous models, incorporating a diverse set of decision variables to address the limitations of prior works. Notably, there is a conspicuous absence of research on integrated green, resilient, and responsive mixed SCND. Consequently, the principal contributions of this research can be delineated as follows:

- Introduction of a pioneering optimization model addressing the complexities of green and resilient mixed SCND.
- Acknowledgment of potential disruptions across all SCN facilities and vehicles, emphasizing comprehensive resilience planning.
- Implementation of various resilience strategies alongside the introduction of a novel approach termed “backup vehicles” to mitigate disruptions effectively.
- Deliberate consideration of both initial SC design and subsequent redesign concepts for enhanced adaptability.
- Introduction of an innovative hybrid metaheuristic solution approach tailored to manage problem intricacies, with a comparative analysis against two other refined hybrid metaheuristics.

3. Problem definition and mathematical modeling

In this section, we delineate the problem scope and present the formulated mathematical model.

3.1 Problem definition

The research explores a complex multi-echelon, multi-period, and multi-product SC network design/redesign problem. This network encompasses a diverse array of entities, including suppliers, factories, DCs, demand zones, collection/inspection centers, recycling centers, and remanufacturing centers. Within this framework, factories manufacture products utilizing raw materials sourced from suppliers. Subsequently, these products undergo distribution, either via DCs to demand zones or directly from factories to demand zones through a dual-channel distribution approach. End-of-life (EOL) products are collected by dedicated centers, where a portion undergoes inspection and is divided for transfer to recycling or remanufacturing centers. Any products unsuitable for recycling or remanufacturing are directed to disposal centers. Remanufacturing centers play a crucial role in converting products into usable variants of the same type, albeit with reduced price and quality compared to newly manufactured counterparts. These remanufactured products are integrated back into the SC network, routed through DCs to reach demand zones. Simultaneously, recycling centers extract raw materials from recycled products, alongside producing recycled products for utilization within this or other SC networks. The extracted raw materials are returned to factories for the production of new goods, while recycled products are dispatched to other SCs. Various types of vehicles facilitate the transshipment of products and materials throughout the network. Considering these parameters and the earlier definition of a mixed SC network, as outlined in the introduction, the structure of the SC network under investigation here encompasses both open and closed-loop components. Fig. 1 provides a schematic depiction of the SC network configuration under examination.

Table 1
Characteristics of the related research

Research	Problem approach		Supply chain characteristics				Network structure			Reverse logistics operations			Decisions							Uncertainty approach	Solution method
	Design	Redesign	Gr	Res	Rsp	Oth	F	OL/CL	Mixed	Col	Rec	Rem	LA	SS	Fl	CF	Pr	VS	Oth		
Peng et al., 2011	✓			✓			✓						✓		✓					SP	MHeu, CS
Azad et al., 2013	✓			✓			✓						✓		✓					--	BD, CS
Sadghiani et al., 2015	✓			✓			✓						✓		✓				✓	RO	CS
Hasani & Khosrojerdi, 2016	✓			✓			✓						✓	✓	✓				✓	RO	MHeu
Jabbarzadeh et al., 2016	✓			✓			✓						✓		✓					RO	LR, CS
Zohal & Soleimani, 2016	✓		✓					✓		✓	✓		✓		✓					––	MHeu, CS
Nurjanni et al., 2017	✓		✓					✓		✓	✓	✓	✓		✓					––	WM, Oth
Fattahi et al., 2017	✓			✓	✓		✓						✓		✓					SP	CS
Soleimani et al., 2017	✓		✓					✓		✓	✓		✓		✓					FP	MHeu, CS
Rezapour et al., 2017	✓			✓		✓	✓						✓		✓	✓	✓			SP	CS
Fahimnia et al., 2018	✓		✓	✓			✓						✓		✓					SP	CS
Ghavamifar et al., 2018	✓			✓		✓	✓						✓		✓		✓		✓	SP	BD, Oth
Ghomi-Avili et al., 2018	✓		✓			✓		✓		✓	✓		✓	✓	✓		✓		✓	PP	CS, Oth
Sabouhi et al., 2018	✓			✓			✓						✓	✓	✓				✓	SP	CS
Rad & Nahavandi, 2018	✓		✓					✓		✓	✓	✓	✓	✓	✓				✓	--	CS
Jabbarzadeh, Fahimnia, & Sabouhi, 2018	✓			✓		✓	✓						✓	✓	✓	✓				SP	CS
Jabbarzadeh, Haughton, & Khosrojerdi, 2018	✓			✓				✓		✓			✓		✓				✓	SP	LR, CS
Mardan et al., 2019	✓		✓					✓				✓	✓	✓	✓					--	BD, CS
Mohammed et al., 2019	✓		✓	✓			✓						✓	✓					✓	FP	EC, CS
Zhen et al., 2019	✓		✓					✓		✓	✓	✓	✓		✓					SP	LR, CS
Yavari & Zaker, 2019	✓		✓	✓				✓		✓		✓	✓		✓				✓	SP	CS, Oth
Sabouhi et al., 2020	✓			✓	✓		✓						✓	✓	✓	✓				SP	BD, CS, Oth
Vali-Siar & Roghanian, 2020	✓	✓		✓					✓				✓	✓	✓	✓	✓			SP, RO	LR, CS
Boronoos et al., 2021	✓		✓					✓		✓	✓	✓	✓		✓	✓			✓	PP	CS, Oth
Gholami-Zanjani et al., 2021	✓			✓			✓						✓		✓	✓				SP	BD, CS
Gholami-Zanjani et al., 2021	✓		✓	✓			✓						✓		✓					SP	Oth, CS
Mehrjerdi & Shafiee, 2021	✓			✓		✓		✓		✓	✓		✓	✓	✓				✓	SP	EC, CS
Hasani et al., 2021	✓		✓	✓			✓						✓	✓	✓				✓	SP, RO	MHeu
Sabouhi et al., 2021	✓			✓		✓	✓						✓	✓	✓	✓			✓	SP, RO	BD
Sazvar et al., 2021	✓			✓		✓	✓						✓	✓	✓	✓				FRO	GP, CS
Fazli-Khalaf et al., 2021	✓			✓		✓		✓		✓	✓	✓	✓		✓					PP	CS
Vali-Siar & Roghanian, 2022	✓			✓		✓			✓	✓	✓	✓	✓	✓	✓	✓			✓	SP, RO	LR, Heu, CS
Yousefi-Babadi et al., 2022		✓		✓			✓						✓	✓	✓					FP, RO	CS
Abbasian et al., 2023	✓		✓	✓			✓						✓		✓		✓	✓	✓	--	Heu, Mheu
Nikian et al., 202		✓	✓	✓				✓		✓					✓					RO	Mheu, LPM, EC
Saeed et al., 2024)	✓		✓	✓		✓		✓		✓	✓		✓	✓	✓	✓	✓			FP	GP
Shekarabi et al., 2024	✓			✓									✓		✓					SP, RO	CS
This paper	✓	✓	✓	✓	✓				✓	✓	✓	✓	✓	✓	✓	✓	✓	✓	✓	**SP**	**MHeu, CS**

SC characteristics: Green (G), Resilient (Res), Responsive (Rsp), Other (Oth)// ***Network Structure***: Forward (F), Open-loop (OL), Closed-loop (CL)// **Reverse logistics operations:** Collection (Col), Recycling (Rec), Remanufacturing (Rm)// ***Decisions***: Location allocation (LA), Supplier selection (SS), Flows of products /materials (Fl), Capacity of facilities (CF), Pricing (Pr), Vehicle selection (VS)// ***Uncertainty approach***: Stochastic programming (SP), Robust optimization (RO), Fuzzy programming (FP), Fuzzy robust optimization (FRO), Robust stochastic possibilistic programming (RSSP)// ***Solution method:*** Heuristic (Heu), Metaheuristic (Mheu), Benders decomposition (BD), Goal programming (GP), LP-metric (LPM), Commercial optimization software (CS), Epsilon-constraint (EC), Weighted sum method (WM), Lagrangian relaxation (LR)

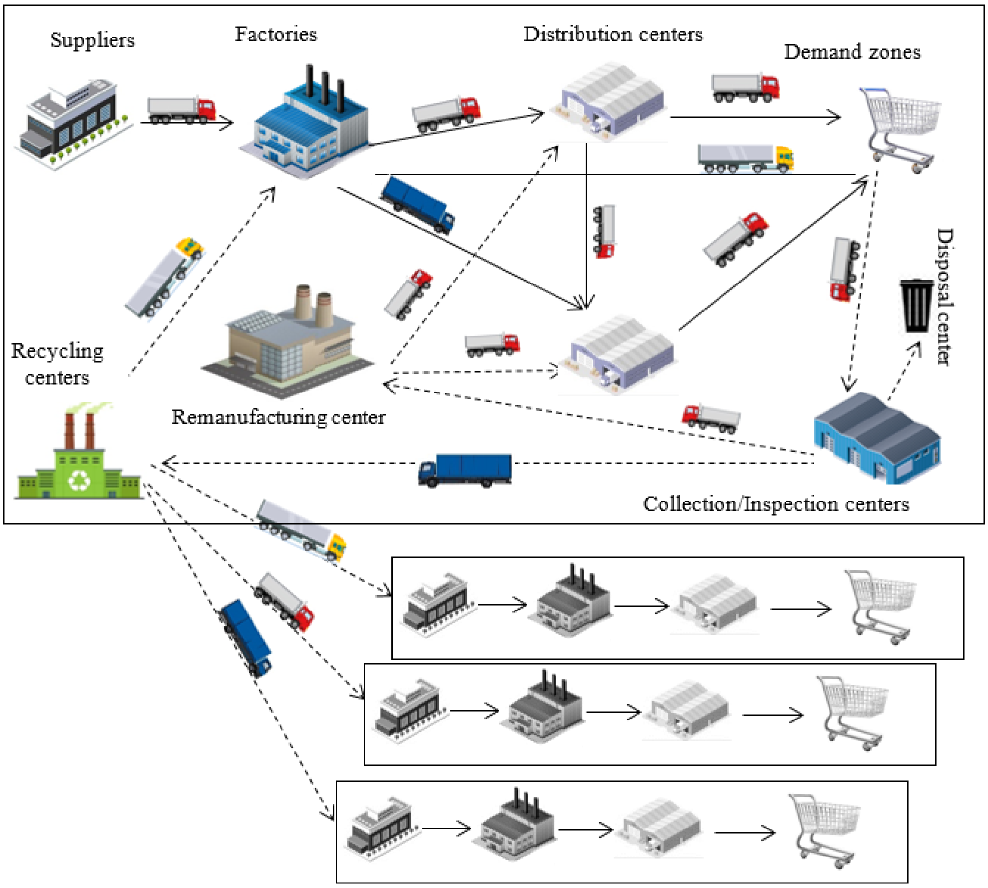

Fig. 1. The network structure of the described supply chain

In our analysis, we consider disruptions impacting both SC facilities and vehicles. Disruptions may result in partial or complete loss of facility capacity. To enhance SC resilience, a range of resilience strategies are proposed, encompassing dual-channel distribution, dynamic pricing, lateral transshipment, facility fortification, integration of backup vehicles supplied by third-party logistics providers, capacity expansion, and multiple sourcing. Dynamic pricing, in particular, serves as a risk mitigation measure, allowing for flexible pricing adjustments across products and demand zones (Yavari & Zaker, 2019). Third-party logistics-provided backup vehicles are intended to mitigate capacity losses incurred by SC vehicles during disruptions. Further elaboration on these strategies is provided in the preceding section. Disruptions not only pose challenges to SC operations but can also impede responsiveness. Thus, responsiveness considerations are integral to the SCND problem. In our approach, responsiveness is addressed by integrating it into the objective function or imposing constraints (Sabouhi et al., 2020). In this study, we adopt the latter approach. Additionally, operational uncertainties regarding production costs of primary products and raw material procurement costs are assumed to exist alongside disruption risks. These uncertainties, whether disruption-related or operational in nature, are addressed through a scenario-based stochastic programming approach. The formulated model encompasses decisions regarding facility establishment/closure, inter-facility flows, and product pricing. Moreover, we assume that demand is influenced by pricing, with a linear correlation between price and demand. To mitigate non-linearity, product prices are discretized. The modeling of this price-demand relationship parallels the approach outlined in Fattahi et al. (2018) , offering further insights for interested readers.

3.2 Mathematical model

To encapsulate the identified problem, a bi-objective MILP model has been constructed. The primary objective aims to maximize the overall profit generated by the SC, while the secondary objective endeavors to minimize adverse environmental effects attributed to SC operations. These environmental impacts encompass greenhouse gas emissions and other detrimental consequences arising from facility establishment and related activities. The model commences with the presentation of sets, parameters, and variables, followed by a detailed exposition of its structure and formulation.

Sets	
I	Set of suppliers, $i \in I$
P	Set of existing and possible locations for factories, $p \in P$. The set of existing factories is denoted by P^0 ($p^0 \in P^0$), and the set of possible locations for factories is denoted by P^n ($p^n \in P^n$). $P = P^n \cup P^0$ and $P^n \cap P^0 = \emptyset$.
J	Set of existing and potential DCs, denoted by j and j'. The set of existing DCs is denoted by J^0 ($j^0 \in J^0$), and the set of potential locations for new DCs is denoted by J^n ($j^n \in J^n$). . $J = J^n \cup J^0$ and $J^n \cap J^0 = \emptyset$.
C	Set of demand zones, $c \in C$
K	Set of possible locations for collection/ inspection centers, $k \in K$
H	Set of possible locations for recycling centers, $h \in H$
R	Set of possible locations for remanufacturing centers, indexed by $r \in R$
G	Set of other SCs, indexed by g
V	Set of vehicle types related to SC and third-party logistics company, $v \in V$. The index of SC vehicle types is denoted by v^0 ($v^0 \in V^0$), and the index of third-party logistics vehicle types is denoted by v^{tpl} ($v^{tpl} \in V^{tpl}$). $V = V^0 \cup V^{tpl}$ and $V^0 \cap V^{tpl} = \emptyset$.
A	Set of fortification levels, $a \in A$
E	Set of product types, $e \in E$
O	Set of capacity levels for DCs and collection/inspection centers, $o \in O$
W	Set of facilities, customers and other SCs $w, w' \in W$, $W = \{i, p, j, c, k, h, r, c, g\}$
L	Set of price levels, $l \in L$
T	Set of time periods, $t \in T$
S	Set of scenarios, $s \in S$

Parameters	
fs_i	Fixed cost of choosing supplier i
fe_{wa}	Establishment cost of facility $w\|w \in \{p, h, r\}$ with fortification level a
fe_w	Establishment cost of facility $w\|w \in \{j, k\}$ with fortification level a
fcl_j	Fixed cost of closing facility j
fcd_{ow}	Fixed cost of developing capacity level o for facility $w\|w \in \{j, k\}$
ψ	Maximum number of existing DCs that can be closed
$tc_{ww'v}$	Unit shipment cost between location w and location w' using vehicle type v
mc_{eps}	Unit production cost of product type e in factory p w under scenario s
ce_{pes}	Unit capacity development cost for product type e in factory p under scenario s
hc_w	Handling cost of products in facility $w\|w \in \{j, k\}$
rc_h	Unit recycling cost in recycling center h
rm_{er}	Unit remanufacturing cost of product type e in remanufacturing center r
dp	Unit disposing cost
cr_{is}	Unit purchase cost of raw material supplied by supplier i under scenario s
ud_{ec}	Unit penalty cost of unmet demand for product type e in demand zone c
udm_{ec}	Unit penalty cost of unmet demand for remanufactured product type e in demand zone c
udr_g	Unit penalty cost of unmet demand for recycled products in SC g
eo_{wa}	Environmental impact caused by opening facility $w\|w \in \{p, h, r\}$ with fortification level a
eo_w	Environmental impact caused by opening facility $w\|w \in \{j, k\}$
ep_{ep}	Environmental impact caused by manufacturing a unit of product type e in factory p
es_e	Environmental impact caused by disposing a unit of product type e or releasing in environment
el_h	Environmental impact caused by processing a unit of product in recycling center h
em_{er}	Environmental impact of processing a unit of product type e in remanufacturing center r
$et_{ww'v}$	Unit environmental impact of transportation between location w and location using vehicle type v
δ	Percentage of obtained recycled materials by recycling one unit of product
dm_{clets}	Demand of demand zone c related to price level l for product type e in period t, under scenario s
dr_{clets}	Demand of demand zone c related to price level l for remanufactured product type e in period t, under scenario s
drc_{glts}	Demand of SC g elated to price level l for recycled products in period t, under scenario s
pr_{lec}	Offered price level l for product type e for selling to demand zone c
pr'_{lec}	Offered price level l for remanufactured product type e for selling to demand zone c
prc_{lg}	Offered price level l for recycled materials for selling to SC g
τ_c	Pre-specified responsiveness level for demand zone c
$\bar{\tau}_g$	Pre-specified responsiveness level for SC g
cp_w	Capacity of facility $w\|w\{i, p, j, k, h, r\}$
cdp_p	Distribution capacity of factory p
cep_p	Maximum capacity that can be added to factory p
cl_{ow}	Capacity level o for facility $w\|w \in \{j, k\}$
cpv_v	Capacity of vehicle type v
nv_{vwt}	Total number of vehicle type v ($v \in V^0$) available for shipping raw materials from facility $w\|w \in \{i, p, j, k, h, r, c\}$ in period t
nvt_{vt}	Total number of vehicle type v ($v \in V^{tpl}$) available for shipping products in SC supplied from third-party logistics company in period t
α_{ce}	Fraction of collected product type e from demand zone c

β_e	Fraction of collected product type e shipped from collection/ inspection centers to remanufacturing centers
γ_e	Fraction of collected product type e shipped from collection/ inspection centers to recycling centers
λ_{wats}	Non-disrupted fraction of manufacturing capacity of facility $w\|w \in \{p,h,r\}$ with fortification level a in period t under scenario s
λ'_{pats}	Non-disrupted fraction of distribution capacity of factory p with fortification level a in period t under scenario s
η_{wts}	Non-disrupted fraction of capacity of facility $w\|w \in \{i,j,k\}$ in period t under scenario s
φ_{vwts}	Available fraction of total number of vehicle type v ($v \in V^0$) for transporting raw materials from facility $w\|w \in \{i,p,j,k,h,r,c\}$ in period t under scenario s
π_s	Probability of scenario s occurrence

Variables	
qr_{ipvts}	Flow of required raw material transferred from supplier i to factory p using vehicle v in period t under scenario s
ma_{epts}	Amount of product type e produced at factory p in period t under scenario s
ac_{pets}	Amount of expanded capacity of factory p for producing product type e in period t Flow scenario s
$qp_{eww'vts}$	Flow of product type e transferred from location w to location w' using vehicle v in period t under scenario s
$qm_{eww'vts}$	Flow of remanufactured product type e transferred from location w to location w' ($w, \in \{r,j,c\}$) using vehicle v in period t under scenario s
f_{hpvts}	Flow of recycled materials transferred from recycling center h to factory p using vehicle v in period t under scenario s
f'_{hgvts}	Flow of recycled materials transferred from recycling center h to SC g using vehicle v in period t under scenario s
ω_{celts}	Amount of unmet demand of demand zone c for product type e with price level l in period t under scenario s
ω'_{celts}	Amount of unmet demand of demand zone c for remanufactured product type e with price level l in period t under scenario s
ω''_{glts}	Amount of unmet demand of SC g with price level l for recycled materials in period t under scenario s
ss_i	1 if supplier i is selected, 0 otherwise
x_{wa}	1 if facility $w\|w \in \{p,h,r\}$ with fortification level a is opened, 0 otherwise.
x_j	1 if facility $w\|w \in \{j,k\}$ is opened, 0 otherwise
x'_j	1 if DC j is closed, 0 otherwise
xcd_{ow}	1 if capacity level o is developed for facility $\|w \in \{j,k\}$, 0 otherwise.
v_{lects}	1 if price level l is selected for product e for selling to demand zone c in period t under scenario s
v'_{lects}	1 if price level l is selected for remanufactured product e for selling to demand zone c in period t under scenario s
v''_{lgts}	1 if price level l is selected for recycled materials for selling to SC G in period t under scenario s

$$Max\ Z_{Ec} = Z_1^R - (Z_1^F + Z_1^T + Z_1^V) \tag{1}$$

$$Z_1^R = \sum_s \pi_s \Big(\sum_l \sum_t \Big(\sum_e \sum_c (v_{lects} dm_{clets} pr_{lec} + v'_{lects} dr_{clets} pr'_{lec} - \omega_{celts} pr_{lec} - \omega'_{celts} pr'_{lec}) + \sum_g (v''_{lgts}\, drc_{lgts} prc_{lg} - \omega''_{glts} prc_{lg})\Big)\Big) \tag{1-1}$$

$$Z_1^F = \sum_i fs_i ss_i + \sum_p \sum_a fe_{pa} x_{pa} + \sum_{j\in J^n} fe_j x_j + \sum_{j\in J^0} fcl_j\,(x'_j) + \sum_k fe_k\, x_k + \sum_h \sum_a fe_{ha}\, x_{ha} + \sum_r \sum_a fe_{ra}\, x_{ra} \tag{1-2}$$

$$\begin{aligned} Z_1^T = \sum_s \pi_s \Big(& \sum_i \sum_p \sum_v \sum_t qr_{ipvts} tc_{ipv} \\ & + \sum_p \sum_j \sum_v \sum_t qp_{epjvts} tc_{pjv} \\ & + \sum_p \sum_c \sum_e \sum_v \sum_t qp_{epcvts} tc_{pcv} \\ & + \sum_j \sum_{j'\neq j} \sum_e \sum_v \sum_t qp_{ejj'vts} tc_{jj'v} \\ & + \sum_j \sum_c \sum_e \sum_v \sum_t (qp_{ejcvts} + qm_{ejcvts}) tc_{jcv} \\ & + \sum_c \sum_k \sum_e \sum_v \sum_t qp_{eckvts} tc_{ckv} \\ & + \sum_k \sum_r \sum_e \sum_v \sum_t qp_{ekrvts} tc_{krv} \end{aligned} \tag{1-3}$$

$$+\sum_{k}\sum_{h}\sum_{e}\sum_{v}\sum_{t} qp_{ekhvts}tc_{khv}$$
$$+\sum_{r}\sum_{j}\sum_{e}\sum_{v}\sum_{t} qm_{erjvts}tc_{rjv}$$
$$+\sum_{h}\sum_{p}\sum_{v}\sum_{t} f_{hpvts}tc_{hpv}$$
$$+\sum_{h}\sum_{g}\sum_{v}\sum_{t} f'_{hgvts}tc_{hgv})$$

$$Z_1^V = \sum_{s}\pi_s (\sum_{i}\sum_{p}\sum_{v}\sum_{t} cr_{is}qp_{ipvts} + \sum_{p}\sum_{e}\sum_{t} mc_{eps}ma_{epts}$$
$$+\sum_{p}\sum_{e}\sum_{t} ce_{pes}ac_{pets} + \sum_{j}\sum_{c}\sum_{e}\sum_{v}\sum_{t} hc_j(qp_{ejcvts} + qm_{ejcvts})$$
$$+\sum_{c}\sum_{k}\sum_{e}\sum_{v}\sum_{t} hc_k qp_{eckvts}$$
$$+\sum_{h}\sum_{v}\sum_{t} rc_h (\sum_{p} f_{hpvts} + \sum_{g} f'_{hgvts})$$
$$+\sum_{r}\sum_{j}\sum_{e}\sum_{v}\sum_{t} rm_{er}qm_{erjvts} \tag{1-4}$$
$$+dp\sum_{e}\sum_{k}\sum_{v}\sum_{t}(\sum_{c} qp_{eckvts} - \sum_{r} qp_{ekrvts} - \sum_{h} qp_{ekhvts})$$
$$+\sum_{o}\sum_{j} cl_{oj}\, xcd_{oj} + \sum_{o}\sum_{k} cl_{ok}\, xcd_{ok}$$
$$+\sum_{c}\sum_{e}\sum_{l}\sum_{t} ud_{ec}\,\omega_{celts}$$
$$+\sum_{c}\sum_{e}\sum_{l}\sum_{t} udm_{ec}\,\omega'_{cets} + \sum_{g}\sum_{l}\sum_{t} udr_g\omega''_{glts})$$

$$Min\ Z_{En} = Z_2^F + Z_2^V + Z_2^T \tag{2}$$

$$Z_2^F = \sum_{p}\sum_{a} eo_{pa}x_{pa} + \sum_{j} eo_j x_j + \sum_{k} eo_k x_k + \sum_{h}\sum_{a} eo_{ha}x_{ha}$$
$$+\sum_{r}\sum_{a} eo_{ra}\, x_{ha} \tag{2-1}$$

$$Z_2^V = \sum_{s}\pi_s (\sum_{p}\sum_{e}\sum_{t} ep_{ep}(ma_{epts} + ac_{pets})$$
$$+\sum_{h}\sum_{v}\sum_{t} el_h (\sum_{p} f_{hpvpts} + \sum_{g} f'_{hgvts})$$
$$+\sum_{r}\sum_{j}\sum_{e}\sum_{v}\sum_{t} em_{er}qm_{erjvts} \tag{2-2}$$
$$+\sum_{e}\sum_{k}\sum_{v}\sum_{t} es_e(\sum_{c} qp_{eckvts} - \sum_{r} qp_{ekrvts} - \sum_{h} qp_{ekhvts})$$

$$Z_2^T = \sum_{s}\pi_s (\sum_{i}\sum_{p}\sum_{v}\sum_{t} qr_{ipvts}et_{ipv}$$
$$+\sum_{p}\sum_{j}\sum_{e}\sum_{v}\sum_{t} qp_{epjvts}et_{pjv}$$
$$+\sum_{p}\sum_{c}\sum_{e}\sum_{v}\sum_{t} qp_{epcvts}et_{pjv} \tag{2-3}$$
$$+\sum_{j}\sum_{j\prime\neq j}\sum_{e}\sum_{v}\sum_{t} qp_{ejj\prime vts}et_{jj\prime v}$$

$$+\sum_{j}\sum_{c}\sum_{e}\sum_{v}\sum_{t}(qp_{ejcvts}+qm_{ejcvts})et_{jcv}$$
$$+\sum_{c}\sum_{k}\sum_{e}\sum_{v}\sum_{t}qp_{eckvts}et_{ckv}$$
$$+\sum_{k}\sum_{r}\sum_{e}\sum_{v}\sum_{t}qp_{ekrvts}et_{krv}$$
$$+\sum_{k}\sum_{h}\sum_{e}\sum_{v}\sum_{t}qp_{ekvts}et_{khv}$$
$$+\sum_{r}\sum_{j}\sum_{e}\sum_{v}\sum_{t}qp_{erjvts}et_{rjv}$$
$$+\sum_{h}\sum_{p}\sum_{v}\sum_{t}f_{hpvpts}et_{hpv}$$
$$+\sum_{h}\sum_{g}\sum_{v}\sum_{t}f'_{hgvts}et_{hgv})$$

The objective function (1) is formulated to maximize the profit of the SC, computed as the aggregate revenue subtracted from the total costs incurred. Revenue generation, as expressed in Eq. (1-1), encompasses income derived from the sale of primary products, remanufactured items, and recycled goods. The costs incurred by the SC are delineated into three categories. Firstly, fixed costs, as delineated in Eq. (1-2), encompass expenses associated with facility establishment or closure and supplier selection processes. Variable costs, outlined in Eq. (1-3), encompass expenses such as production, raw material procurement, remanufacturing, disposal, recycling, and costs incurred due to unmet demands. Additionally, transportation costs, as depicted in Eq. (1-4), are incorporated.

Objective function (2) aims to minimize the adverse environmental impacts attributed to SC operations. These impacts encompass the environmental consequences arising from facility establishment, product manufacturing, remanufacturing, recycling, disposal, and transportation activities. The environmental effects associated with facility opening are quantified by Eq. (2-1). Eq. (2-2) calculates the environmental impacts stemming from product manufacturing, remanufacturing, recycling, and disposal processes. Additionally, Eq. (2-3) computes the negative environmental effects of transportation activities.

$$\sum_{a}x_{pa}\leq 1 \qquad \forall p\in p^{n} \tag{3}$$
$$\sum_{a}x_{pa}=1 \qquad \forall p\in p^{0} \tag{4}$$
$$\sum_{a}x_{ha}\leq 1 \qquad \forall h \tag{5}$$
$$\sum_{a}x_{ra}\leq 1 \qquad \forall r \tag{6}$$

Only a single fortification level can be selected for the establishment of factories, recycling centers, and remanufacturing centers, as specified by Constraints (3), (5), and (6). Constraint (4) pertains to the maintenance of existing factories, ensuring their continued operation.

$$x_j'=1-x \qquad \forall j\in j^{0} \tag{7}$$
$$\sum_{j\in j^{0}}x_j'\leq \psi \tag{8}$$

Constraint (7) calculates the variable, which plays a role in the formulation of the first objective function. Constraint (8) imposes a restriction on the maximum number of DCs that can be closed.

$$\sum_{i}\sum_{v}qr_{ipvts}+\sum_{h}\sum_{v}f_{hpvts}=ma_{epts}+ac_{pets} \qquad \forall p,t,s \tag{9}$$

Constraint (9) dictates that the requisite raw materials are provided by both suppliers and recycling centers.

$$ma_{epts} + ac_{pets} - \sum_{c}\sum_{v} qp_{epcvts} = \sum_{j}\sum_{v} qp_{epjvts} \qquad \forall p,e,t,s \tag{10}$$

$$\sum_{p}\sum_{v} qp_{epjvts} + \sum_{j\prime\neq j}\sum_{v} qp_{ej\prime jvts} = \sum_{j\prime\neq j}\sum_{v} qp_{ejj\prime vts} + \sum_{c}\sum_{v} qp_{ejcvts} \qquad \forall j,e,t,s \tag{11}$$

$$\sum_{j}\sum_{v} qp_{ejcvts} + \sum_{p}\sum_{v} qp_{epcv1s} + \sum_{l} \omega_{celts} = \sum_{l} dm_{clets}\upsilon_{lects} \quad \forall e,c,t,s \tag{12}$$

Constraints (10)-(12) ensure the equilibrium of forward flows within the SCN. The process of product transportation has been elucidated in the preceding sections of this segment.

$$\sum_{l} \upsilon_{lects} = 1 \quad \forall c,e,t,s \tag{13}$$

$$\sum_{l} \upsilon'_{lects} = 1 \quad \forall c,e,t,s \tag{14}$$

$$\sum_{l} \upsilon''_{lgts} = 1 \quad \forall g,t,s \tag{15}$$

The stipulation that only a single price level may be chosen for each product, scenario, and period is enforced by Constraints (13)-(15).

$$\omega_{celts} \leq dm_{clets}\upsilon_{lects} \quad \forall c,e,l,t,s \tag{16}$$

$$\omega'_{celts} \leq dr_{clets}\upsilon'_{lects} \quad \forall c,e,l,t,s \tag{17}$$

$$\omega''_{glts} \leq drc_{glts}\upsilon''_{lgts} \quad \forall g,l,t,s \tag{18}$$

Constraints (16)-(18) ensure that the quantity of unfulfilled demand remains equal to or less than the demand associated with the chosen price level.

$$\sum_{k}\sum_{v} qp_{eckvts} \leq \alpha_{ce}(\sum_{j}\sum_{v} qp_{ejcvts} + \sum_{p}\sum_{v} qp_{epcvts}) \qquad \forall e,c,t,s \tag{19}$$

$$\sum_{r}\sum_{v} qp_{ekrvts} \leq \beta_{e} \sum_{c}\sum_{v} qp_{eckvts} \qquad \forall e,k,t,s \tag{20}$$

$$\sum_{h}\sum_{v} qp_{ekhvts} \leq \gamma_{e} \sum_{c}\sum_{v} qp_{eckvts} \qquad \forall e,k,t,s \tag{21}$$

$$\sum_{j}\sum_{v} qm_{erjvts} = \sum_{k}\sum_{v} qp_{ekrvts} \qquad \forall e,r,t,s \tag{22}$$

$$\sum_{c}\sum_{v} qm_{ejcvts} = \sum_{r}\sum_{v} qm_{erjvts} \qquad \forall e,j,t,s \tag{23}$$

$$\sum_{p}\sum_{v} f_{hpvpts} + \sum_{g}\sum_{v} f'_{hgvts} = \delta \sum_{e}\sum_{k}\sum_{v} qp_{ekhvts} \qquad \forall h,t,s \tag{24}$$

$$\sum_{j}\sum_{v} qm_{ejcvts} + \sum_{l} \omega'_{celts} = \sum_{l} dr_{clets}\upsilon'_{lects} \qquad \forall c,e,t,s \tag{25}$$

$$\sum_{h}\sum_{v} f'_{hgvts} + \sum_{l} \omega''_{glts} = \sum_{l} drc_{glts}\upsilon''_{lgts} \qquad \forall g,t,s \tag{26}$$

Constraints (19)-(26) uphold the equilibrium of reverse flows within the SC.

$$\sum_{p}\sum_{v} qr_{ipvts} \leq \eta_{its}cp_{i}ss_{i} \qquad \forall i,t,s \tag{27}$$

$$\sum_{e} ma_{epts} \leq cp_{p} \sum_{a} \lambda_{pats}x_{pa} \qquad \forall p,t,s \tag{28}$$

$$\sum_{e}\sum_{c}\sum_{v} qp_{epcvts} \leq cdp_{p} \sum_{a} \lambda'_{pats}x_{pa} \qquad \forall p,t,s \tag{29}$$

$$\sum_{e} ac_{pets} \leq cep_{p} \sum_{a} x_{pa} \qquad \forall p,t,s \tag{30}$$

$$\sum_{o} xcd_{oj} \leq x_j \qquad \forall j \tag{31}$$

$$\sum_{o} xcc_{ok} \leq x_k \qquad \forall j \tag{32}$$

$$\sum_{c}\sum_{e}\sum_{v}(qp_{ejcvts} + qm_{ejcvts}) \leq \eta_{jts}(cp_j x_j + \sum_{o} cl_{oj} xcd_{oj}) \qquad \forall j,t,s \tag{33}$$

$$\sum_{c}\sum_{e}\sum_{v} qp_{eckvts} \leq \eta_{kts}(cp_k x_k + \sum_{o} cl_{ok} xcd_{ok}) \qquad \forall k,t,s \tag{34}$$

$$\sum_{p}\sum_{v} f_{hpvts} + \sum_{g}\sum_{v} f'_{hgvts} \leq cp_h \sum_{a} \lambda_{hats} x_{ha} \qquad \forall h,t,s \tag{35}$$

$$\sum_{e}\sum_{j}\sum_{v} qm_{erjvts} \leq \sum_{a} \lambda_{rats} cp_r\, x_{ra} \qquad \forall r,t,s \tag{36}$$

The capacity limits of SC facilities are ensured not to be exceeded by Constraints (27)-(36), considering the impact of disruptions. It is dictated by these constraints that only one capacity level can be chosen for expanding the capacity of each DC and each collection center, as specified in Constraints (32) and (33) respectively.

$$\sum_{p} qr_{ipvts} \leq \varphi_{vits} cpv_v nv_{vit} \qquad \forall i, v \in v^0, t, s \tag{37}$$

$$\sum_{e}\sum_{j} qp_{epjvts} + \sum_{e}\sum_{c} qp_{epcvts} \leq \varphi_{vpts} cpv_v nv_{vpt} \qquad \forall p, v \in v^0, t, s \tag{38}$$

$$\sum_{e}\sum_{j'} qp_{ejj'vts} + \sum_{e}\sum_{c}(qp_{ejcvts} + qm_{ejcvts}) \leq \varphi_{vjts} cpv_v nv_{vjt} \qquad \forall j, v \in v^0, t, s \tag{39}$$

$$\sum_{e}\sum_{k} qp_{eckvts} \leq \varphi_{vcts} cpv_v nv_{vct} \qquad \forall c, v \in v^0, t, s \tag{40}$$

$$\sum_{e}\sum_{r} qp_{ekrvts} + \sum_{e}\sum_{h} qp_{ekhvts} \leq \varphi_{vkts} cpv_v nv_{vkt} \qquad \forall k, v \in v^0, t, s \tag{41}$$

$$\sum_{e}\sum_{j} qm_{erjvts} \leq \varphi_{vrts} cpv_v nv_{vrt} \qquad \forall r, v \in v^0, t, s \tag{42}$$

$$\sum_{p} f_{hpvts} + \sum_{g} f'_{hgvts} \leq \varphi_{vhts} cpv_v nv_{vht} \qquad \forall h, v \in v^0, t, s \tag{43}$$

$$\begin{aligned} &\sum_{i}\sum_{p} qr_{ipvts} + \sum_{e}\sum_{p}\sum_{j} qp_{epjvts} + \sum_{e}\sum_{p}\sum_{c} qp_{epcvts} \\ &+ \sum_{e}\sum_{j}\sum_{j'} qp_{ejj'vts} + \sum_{e}\sum_{j}\sum_{c}(qp_{ejcvts} + qor_{ejcvts}) \\ &+ \sum_{e}\sum_{c}\sum_{k} qp_{eckvts} + \sum_{e}\sum_{k}\sum_{r} qp_{ekrvts} \\ &+ \sum_{e}\sum_{k}\sum_{h} qp_{ekhvts} + \sum_{e}\sum_{r}\sum_{j} qm_{erjvts} \\ &+ \sum_{h}\sum_{p} f_{hpvts} + \sum_{h}\sum_{g} f'_{hgvts} \leq cpv_v nvt_{vt} \qquad \forall v \in v^{tpl}, t, s \end{aligned} \tag{44}$$

Constraints (37)-(44) outline the restrictions on the capacity of SC vehicles.

$$\frac{\sum_j \sum_e \sum_v qp_{ejcvts} + \sum_e \sum_p \sum_v qp_{epcvts}}{\sum_e \sum_l d_{clets}\, v_{lects}} \geq \tau_c \qquad \forall c,t,s \tag{45}$$

$$\frac{\sum_e \sum_j \sum_v qm_{ejcvts}}{\sum_e \sum_l dr_{clets}\, v'_{lects}} \geq \tau_c \qquad \forall c,t,s \tag{46}$$

$$\frac{\sum_h \sum_{u_2} \sum_v f'_{hgvts}}{\sum_l drc_{glts} v''_{lgts}} \geq \bar{\tau}_g \qquad \forall g,t,s \tag{47}$$

Constraints (45)-(47) are imposed to enforce limitations on the minimum level of responsiveness exhibited by the SC, specifically concerning the proportion of fulfilled demands.

$$qr_{ipvts}, ma_{epts}, ac_{pets}, qp_{eww'vts} \tag{48}$$

$qor_{ejww'ts}, f_{hpvpts},$
$f'_{hgvts}, \omega_{celts}, \omega'_{celts}, \omega''_{glts} \geq 0$
$ss_i, x_{wa}, x_w, xcd_{ow}, \upsilon_{lects}, \upsilon'_{lects}, \upsilon''_{lgts} \in \{0,1\}$
The types of variables are determined by Constraint (48).

4. Solution methods

The NP-hard nature of the SCND problem is acknowledged (Govindan et al., 2016). Likewise, the closed-loop SCND problem is often deemed more intricate than the forward SC design problem, also proven to be NP-hard (Soleimani & Kannan, 2015). Furthermore, the problem presented in this paper has a more complex structure than the closed-loop SCND problem. Therefore, exact optimization methods are not applicable for solving medium and large-sized problems.
To address this challenge, three hybrid metaheuristics have been developed in this study to manage problem complexity and attain high-quality solutions. These include an improved hybrid genetic and particle swarm optimization algorithm (hybrid GA-PSO), an improved hybrid genetic and simulated annealing algorithm (hybrid GA-SA), and a novel hybrid algorithm named hybrid ant colony optimization and teaching and learning-based optimization algorithm (hybrid ACO-TLBO). Additionally, the augmented ε-constraint method, as proposed by Mavrotas (2009), is employed to validate these algorithms.

4.1 Encoding and Decoding

Different methods exist for representing and encoding solutions, with two main approaches being the matrix representation approach (Michalewicz et al., 1991) and the priority-based representation approach (Gen et al., 2006). In this paper, the representation method utilized is akin to the priority-based representation. An example is provided to demonstrate how solutions are represented. The quantities of suppliers, factories, DCs, demand zones, collection centers, recycling centers, remanufacturing centers, and other SCs are 2, 2, 2, 3, 2, 2, 2, and 2, respectively. There are three time periods, and four types of vehicles ($V^0 = \{1,2,3\}$, and $V^{tpl} = \{4\}$). The chromosome comprises two sub-chromosomes. The first sub-chromosome dictates the sequence of transportation between various facilities and specifies the vehicles for transshipping materials and products. As depicted in Fig. 2, the first sub-chromosome is segmented into eight sections based on the flows depicted in Fig. 1. Values inputted in this segment are random numbers ranging between (0, 1). Subsequently, these values are arranged in ascending order for each sub-segment to form the priority-based matrix. The section pertaining to vehicles is populated with random numbers within the range $[1, |V|]$.

Period	Segment 1					Segment 2							
	i		*p*		*v*	*p*		*j+c*					*v*
1	0.23	0.88	0.90	0.38	2	0.35	0.31	0.18	0.72	0.56	0.96	0.11	2
2	0.83	0.50	0.79	0.11	2	0.81	0.12	0.32	0.00	0.06	0.50	0.88	1
3	0.85	0.74	0.49	0.79	1	0.45	0.57	0.41	0.40	0.29	0.10	0.27	3

Period	Segment 3						Segment 4					
	j		*c*			*v*	*c*			*k*		*v*
1	0.46	0.34	0.89	0.60	0.73	1	0.52	0.49	0.03	0.32	0.46	4
2	0.10	0.52	0.17	0.88	0.81	1	0.50	0.66	0.26	0.74	0.20	3
3	0.05	0.35	0.97	0.06	0.58	2	0.07	0.62	0.78	0.95	0.65	3

Period	Segment 5							Segment 6				
	k		*r+h*				*v*	*r*		*j*		*v*
1	0.79	0.15	0.60	0.52	0.40	0.47	3	0.88	0.82	0.74	0.39	1
2	0.23	0.11	0.00	0.93	0.20	0.44	2	0.59	0.80	0.21	0.32	3
3	0.23	0.69	0.64	0.76	0.48	0.77	1	0.75	0.55	0.16	0.33	1

Period	Segment 7						Segment 8					
	j		*c*			*v*	*h*		*p+g*			
1	0.56	0.92	0.18	0.84	0.58	2	0.86	0.62	0.78	0.03	0.10	0.14
2	0.87	0.78	0.74	0.40	0.34	4	0.90	0.34	0.01	0.26	0.60	0.04
3	0.48	0.81	0.57	0.63	0.68	3	0.86	0.94	0.23	0.78	0.82	0.13

Fig. 2.a. The graphical illustration of the first sub-chromosome

		e=1	e=2
t=1	c=1	1	4
	c=2	4	2
t=2	c=1	3	1
	c=2	5	2

		e=1	e=2
t=1	c=1	2	3
	c=2	1	1
t=2	c=1	4	5
	c=2	2	2

t=1	g=1	1
	g=2	4
t=2	g=1	3
	g=2	5

Fig. 2.b. The graphical illustration of the second sub-chromosome
Fig. 2. The graphical illustration of the proposed chromosome

To enhance the explanation of the solution representation, segment 2 of the first sub-chromosome is elaborated upon in greater detail. Fig. 3 illustrates the priority-based chromosome of this segment in period 1. Like other segments, the second segment comprises two sub-segments. This segment pertains to the transshipment of products from factories (p) to DCs (j) and demand zones (c). The first and second columns of sub-segment 2 correspond to DCs, while the third to fifth columns relate to demand zones. The final column of this segment displays the chosen type of vehicle for transporting product flows. It is observed that the random values of the chromosome are independently sorted for each sub-segment, determining the allocation order accordingly. For instance, if factory 2 is established (as per segment 1), products are initially shipped from this center to demand zone 1; otherwise, factory 2 is selected. Notably, constraints (7), (8), (10), (29), (31), and (33) must be taken into account in this described procedure. The values of variables associated with product flow from factories to DCs and demand zones, as well as the binary variable corresponding to the establishment of DCs, are determined based on this segment. To streamline the explanation, a pseudo-code is presented in Fig. 4, depicting the general decoding procedure. Such a procedure must be implemented for all segments, with differences in details and consideration of the relevant constraints.

The second sub-chromosome comprises three sectors. The first sector specifies the price level of the main products, while the second and third sectors determine the price level of the remanufactured and recycled products, respectively. Each sector's cells are populated with random numbers within the range [1, |L|].

p		j+c				
2	1	2	4	3	5	1

Fig. 3. The graphical illustration of priority-based chromosome of segment 2 in period 1

Inputs: Sets and parameters of the problem
Outputs: Decision variables
Begin:
Step 0. (initialization)
$\bar{I}$: set of source facility
$\bar{J}$: set of applicant
Let ϱ denote the set of distribution centers and collection centers and $XC_{o\varrho}$ denote the binary variables related to determining the capacity level
Let cm denote the first sub-chromosome
$\bar{D}_{j,s}$: demand of applicant j under scenario s
$\overline{Ca}_{i,s}$: capacity of source facility under scenario s
prb_{nbmt}: The element m of sub-segment b ($b \in \{1,2\}$) of segment n ($n \in \{1,2,\dots,8\}$) in priority based vector related to period t (prb: the prioirity based matrix)
Let $\bar{X}_i$ and $\bar{Y}_j$ denote binary variables which show whether source facility or applicant is opened or not.
Let w denote the set of production centers, recycling centers and manufacturing centers and let $\bar{X}_{wau}$ is equal to 1 if fortification level a and technology u is selected for facility w
Let XF_{ij}^{s} denote the material/ product flow between source i and applicant j under scenario s
If the status of $\bar{X}_i$ is specified in computations of last segments or is predetermined, then delete the elements which their corresponding value in $\bar{X}_i$ is zero.
If the status of $\bar{Y}_i$ is specified in computations of last segments or is predetermined, then delete the elements which their corresponding value in $\bar{Y}_i$ is zero.
Step 1.
for i=1:|S| **do**
Select a scenario randomly (s)
for t=1:|T| **do**
$\overline{prb}_{nbm}=prb_{nbmt}$;
while $\sum_m \overline{Ca}_{prb_{n1m,s}} > 0$ and $\sum_m \bar{D}_{prb_{n2m,s}} > 0$
$XF^{s}_{\overline{prb}_{n11}\,\overline{prb}_{n21}} = min(\bar{D}_{\overline{prb}_{n21,s}}, \overline{Ca}_{\overline{prb}_{n11,s}})$;
$\overline{Ca}_{\overline{prb}_{n11,s}} = \overline{Ca}_{\overline{prb}_{n11,s}} - XF^{s}_{\overline{prb}_{n11}\,\overline{prb}_{n21}}$;
$\bar{D}_{\overline{prb}_{n21,s}} = \bar{D}_{\overline{prb}_{n21,s}} - XF^{s}_{\overline{prb}_{n11}\,\overline{prb}_{n21}}$;
if $\overline{prb}_{nb1} \in \varrho$ & $i = 1$
$o = min\{|O|, \lceil 1/\, cm_{\overline{prb}_{nb1}} \rceil\}$;
$XC_{o\varrho} = 1$;
end
if $\overline{prb}_{nb1} \in w$ & $i = 1$
$a = min\{|A|, \lceil 1/\, cm_{\overline{prb}_{nb1}} \rceil\}$;
Randomly select n' ($n' \in n$);
$u = min\{|U|, \lceil 1/\, cm_{\overline{prb}_{n'b1}} \rceil\}$;
$\bar{X}_{wau} = 1$;
end
if $i = 1$
$\bar{X}_{|\overline{prb}_{n11}}=1|\overline{prb}_{n11} \notin C$; $\bar{Y}_{\overline{prb}_{n21}}=1|\overline{prb}_{n21} \notin C, G$;
end
if $\overline{Ca}_{\overline{prb}_{n11}} = 0$
$\overline{prb}_{n11} = []$;
end
if $\bar{D}_{\overline{prb}_{n21}} = 0$
$\overline{prb}_{n21} = []$;
end
end
end
end
end
Report Decision variables

Fig. 4. Pseudo-code of decoding procedure

4.2 Multi-objective hybrid ACO-TLBO

Ant colony optimization (ACO), introduced by (Dorigo, 1992) and subsequently developed further by Dorigo et al. (1996) and Dorigo et al. (1999) , draws inspiration from the foraging behavior of ants in nature. When an ant finds food, it carries it back to the nest, leaving a trail of pheromones along the way. This pheromone trail helps other ants locate the food, with the amount of pheromone being proportional to the quality and quantity of the food found (Socha & Dorigo, 2008). ACO has been widely utilized as a combinatorial optimization tool in various studies, including SCND, as demonstrated by the works of Moncayo-Martínez & Zhang (2011), and Bottani et al. (2019).

Despite numerous attempts to adapt ACO for continuous domains, these efforts largely failed to maintain the integrity of the original algorithm. However, Socha & Dorigo (2008) successfully extended the ACO metaheuristic to continuous domains without altering its core principles. This adaptation, known as ACO for continuous optimization (ACOR), proves effective for solving mixed discrete-continuous problems, such as the one explored in this paper.

The ACOR algorithm begins with the construction of solutions by ants. Initially, n_{pop} (archive size) random solutions ($s_l, l \in \{1, \dots, n_{pop}\}$) are generated, evaluated, and sorted based on their objective function values from best to worst. These solutions and their corresponding objective function values are stored in a solution archive. Subsequently, a weight coefficient is calculated for each solution.

To generate new solutions in the algorithm's main loop, a continuous probability distribution function (PDF) is utilized, differing from the discrete ACO. This PDF is constructed based on the solutions stored in the archive. An ant selects one solution from the archive based on a probability distribution. For sampling and constructing new solutions, Socha & Dorigo (2008) proposed using a Gaussian function as the PDF. The PDF related to each dimension i of the problem for solution l is denoted by g_l^i. The Gaussian kernel, defined as a weighted sum of one-dimensional Gaussian functions g_l^i, is used to sample and construct new solutions.

$$G^i(x) = \sum_{l=1}^{n_{pop}} p_l g_l^i(x) = p_l \frac{1}{\sigma_i^l \sqrt{2\pi}} e^{-\frac{(x-s_l^i)}{2\sigma_i^{l^2}}} \tag{49}$$

Where the probability p_l of selecting solution l is calculated using the following formula:

$$p_l = \frac{w_l}{\sum_{m=1}^{n_{pop}} w_m} \tag{50}$$

The weight of solution l, denoted as w_l, can be determined using the following equation:

$$w_l = \frac{1}{q n_{pop} \sqrt{2\pi}} e^{-\frac{(l-1)}{2q^2 n_{pop}^2}} \tag{51}$$

As outlined earlier, the solution s_l holds a rank of l, where q represents one of the algorithm's parameters. As q diminishes there is an augmented inclination towards selecting solutions with superior ranks. This tendency is encapsulated in Equation (51), which indicates that an elevated solution weight correlates with an increased likelihood of sampling in its proximity. The determination of the standard deviation σ_i^l involves computing the average distance between solution s_l^i and other solutions within the archive. Subsequently, the sampling of the designated Gaussian function can be executed utilizing a random number generator capable of producing random numbers conforming to a standard normal distribution (Socha & Dorigo, 2008)

$$\sigma_i^l = \zeta \sum_{m=1}^{n_{pop}} \frac{|s_m^i - s_l^i|}{n_{pop} - 1} \tag{52}$$

The parameter ζ, being a positive value, operates analogously to the pheromone evaporation rate characteristic of the Ant Colony Optimization (ACO) algorithm.

The second stage of the ACOR algorithm encompasses the Pheromone Update process, wherein the solution archive incorporates pheromone information (Liao et al., 2013; Socha & Dorigo, 2008). This update mechanism involves generating new solutions and integrating them into the solution archive. Subsequently, the newly generated solutions are amalgamated into the archive, necessitating a re-sorting of solutions. It is imperative to maintain a constant archive size throughout the algorithm's execution, thereby requiring the removal of additional solutions of inferior quality compared to others. As the quality of solutions stored in the archive improves, it enhances the efficacy of guiding ants within the search space. This iterative process persists until the stipulated termination condition is satisfied.

The TLBO algorithm, introduced by Rao et al. (2011), has garnered widespread adoption in various scientific and engineering domains due to its demonstrated efficacy in solving optimization problems (Rajesh, 2020). Consisting of two distinct phases—the teacher phase and the learner phase—TLBO operates as a population-based algorithm. Initially, a population of n_{pop} solutions is randomly generated. During the teacher phase, the algorithm learns from a teacher, where

$sol_{i,it}$ denotes the solution generated in iteration it associated with solution i, and Mn_{it} signifies the mean of solutions within the population at iteration it. The teacher at iteration it is identified as the best solution attained up to that iteration, denoted by T_{it}. The derivation of the new solution $sol_{i,it}^{new}$ is determined as follows:

$$sol_{i,it}^{new} = sol_{i,it} + r(T_{it} - TF * Mn_{it}) \tag{53}$$

In this contex, r represents a randomly generated number within the interval [0, 1], while TF is a random selection between 1 and 2. If the newly proposed solution demonstrates superior fitness compared to the existing solution, it supersedes the latter.

In the learner phase, the refinement of learners (solutions) is facilitated through interactions among themselves. During each iteration of this phase, for every solution i, another solution j $(i \neq j)$ is randomly chosen. Subsequently, a comparison is made between these solutions based on their fitness values, and the solution i. Solution i undergoes adjustment based on the following procedure:

If $sol_{i,it}$ is better than $sol_{j,it}$
$$sol_{i,it}^{new} = sol_{i,it} + r(sol_{i,it} - sol_{j,it})$$
else (54)
$$sol_{i,it}^{new} = sol_{i,it} - r(sol_{i,it} - sol_{j,it})$$
end

The replacement of the previous solution occurs when the new solution exhibits a superior fitness value. The amalgamation of the ACOR and TLBO algorithms, as conducted in this study, appears to be unprecedented in existing literature. When formulating the structure of the hybrid algorithm, it is crucial to consider the multi-objective nature of the problem under investigation and devise an appropriate approach to address this complexity. Presented in Fig. 5 is the pseudo-code outlining the hybrid ACO-TLBO algorithm. Initially, the solution archive is randomly generated, and computations for solution weights and selection probabilities are performed. Given the bi-objective nature of the problem, the non-dominated sorting algorithm, introduced by Deb et al. (2002), is employed prior to initiating the primary loop. Within this loop, the algorithm executes the ACO steps initially, followed by the application of the non-dominated sorting algorithm. The resulting first front from this sorting process is designated as teachers, and teaching operations ensue. Subsequently, the learning phase is executed. Finally, following the merging of new solutions with the primary population, the non-dominated sorting algorithm is applied once more. The best Pareto solutions are then reported upon meeting the stipulated termination criterion.

Inputs: Sets and parameters of the problem
Outputs: Decision variables and the best non-dominated solutions
Begin:
Step 0. (initialization)
Generate n_{pop} (archive size) solutions randomly, apply decoding procedure, evaluate the solutions (calculate both objectives) and store them in the solution archive
Apply non-dominated sorting
Compute the vector of solution weights (equation 51)
Compute the vector of selection probability of the solutions (equation 50)
Step 1. (Hybrid ACO-TLBO main loop)
for $it = 1$: *Max-iteration*
%ACO operations
for $l = 1{:}\, n_{pop}$
$\sigma^l = \zeta \sum_{m=1}^{n_{pop}} \frac{|sol_m - sol_l|}{n_{pop} - 1}$ (computing the matrix of standard deviations)
for j=1: n_{sample}
Select a random solution by roulette wheel selection (solution P)
rn=randomly generate a random normal number with mean 0 and standard deviation 1
$sol_j^{new} = sol_p + \sigma^l\, rn$
end
Merge main and new population and apply non-dominated sorting
%TLBO operations (teacher phase)
Set the first front of non-dominated solutions as teachers (Let n_t denote the number of teachers)
compute the mean of the population solutions
for $i = 1{:}\, n_t$
for $j = 1{:}\, n_{pop}$
Let r a random number in range [0, 1] and TF a randomly selected number which can be either 1 or 2
$sol_j^{new} = sol_j + r(T_i - TF * Mn)$
end
end
$j = n_t + 1$
%TLBO operations (learner phase)
for $i = 1{:}\, n_{pop}$
randomly select a solution $(k, k \neq i)$
Let r a random number in range [0, 1]
if $f_1(sol_i) > f_1(sol_k)$ && $f_2(sol_i) < f_2(sol_k)$
$sol_j^{new} = sol_i + r(sol_i - sol_k)$
else if $f_1(sol_i) \leq f_1(sol_k)$ & $f_2(sol_i) \geq f_2(sol_k)$
$sol_j^{new} = sol_i - r(sol_i - sol_k)$
else randomly select b that can be either -1 or +1
$sol_j^{new} = sol_i + s * r(sol_i - sol_k)$
end
end
Merge main population and new solutions and apply non-dominated sorting and remove redundant solutions (size of archives is n_{pop})
end
Report best found Pareto solutions

Fig. 5. Pseudo-code of multi-objective hybrid ACO-TLBO algorithm

The multi-objective hybrid ACO-TLBO algorithm harnesses the inherent foraging behavior of ants and the principles of teaching and learning. Essentially, the process mirrors ants' quest for food, wherein their exploration aids in updating the pheromone trails (represented by the solution archive) and engaging in teacher-learner interactions to refine the solutions further.

4.3 Multi-objective hybrid improved GA-PSO

Holland (1975) developed developed the genetic algorithm (GA), while Kennedy & Eberhart (1995) introduced the particle swarm optimization (PSO).

```
Inputs: Sets and parameters of the problem
Outputs: Decision variables and the best non-dominated solutions
Begin:
  Step 0. (initialization)
  Generate n_pop solutions randomly, apply decoding procedure and evaluate the solutions (calculate both
  objectives) and store them in pop
  nc=pc*npop (number of parents for doing crossover), nm=pm*npop (number of mutants)
  let pop, popc and popm be the vacant population related to initial solutions, solutions affected by crossover
  and mutation
  Apply non-dominated sorting and crowding distance procedures
  Step 1. (Hybrid GA-PSO main loop)
  for it = 1: Max-iteration
  %GA operations
    for i = 1: n_c/2
      Select the crossover type randomly
      Select two solutions (parents) randomly from population
      Apply crossover on the selected parents and obtain offsprings
      Apply decoding procedure and evaluate the solutions and store the solutions in pop_c
    end
    Merge pop_c and pop and apply non-dominated sorting and crowding distance procedures
    store n_e number of best solutions (elites) in elites archive (pop_e)
    for i = 1: n_m
      Select a solution randomly from population
      Apply mutation containing local search
      Apply decoding procedure and evaluate the solutions and store the solutions in pop_m
    end
    Apply non-dominated sorting and crowding distance procedures
    for i = 1: n_m
      Compare the solution i of pop_m with solution the first solution of pop_e
      If solution i is dominated
        Replace sol_i of pop_m with sol_i^e of pop_e and remove the first solution of pop_e
        If pop_e = []
          Break the loop
        end
      end
    end
    Merge pop_c, pop_m and pop and apply non-dominated sorting and crowding distance procedures
    Save n_pop number of best solutions and remove others
    %PSO operations
    for i = 1: n_pop
      If it = 1
        sol_i.velocity = zero matrix
        sol_i^best.position = sol_i.position
        sol_i^best.cost = sol_i.cost
      end
      Select a leader randomly for sol_i from the first front of non-dominated solutions
      sol_i.velocity = w_1 * sol_i.velocity + c_1 * rand * (sol_i^best.position - sol_i.position)+ c_2 *
      rand * (sol_i^leader.position - sol_i.position)
      sol_i.position = sol_i.position + sol_i.velocity
      if sol_i.position dominates sol_i^best.position
        sol_i^best.position = sol_i.position
        sol_i^best.cost = sol_i.cost
      else if sol_i^best and sol_i does not dominate each other
        Randomly select sol_i^best or sol_i as the sol_i^best
      end
    end
    apply non-dominated sorting and crowding distance procedures
  end
Report best found Pareto solutions
```

Fig. 6. Pseudo-code of multi-objective hybrid improved GA-PSO

Both algorithms are widely recognized metaheuristics known for their effectiveness in solving optimization problems across various domains. The amalgamation of GA and PSO, a well-established approach in the literature, has exhibited notable performance in optimization tasks (Soleimani & Kannan, 2015). In this study, we propose the multi-objective hybrid improved GA-PSO as an alternative solution method. To address the multi-objective nature of the problem, we adopt the non-dominated sorting approach proposed by Deb et al. (2002). The pseudo-code detailing the algorithmic procedure is provided in Fig. 6. Initially, a population of n_{pop} solutions is randomly generated. Subsequently, the GA operations are executed. Within the GA framework, two additional steps are incorporated. Firstly, a set of n_e elite solutions, representing the best-performing individuals after crossover, are preserved. These elite solutions may replace dominated solutions generated by the mutation operator, thereby enhancing population quality and expediting the acquisition of a high-quality Pareto set. Secondly, a local search mechanism is embedded within the mutation operator. This mutation involves the random selection of two columns within the chromosome, followed by pairwise swapping. The solution is then adjusted based on the optimal displacement obtained. Three types of crossover operations, namely single-point, double-point, and uniform, are employed. Following the execution of GA operators, the PSO operations are initiated. This iterative process continues until the specified stopping criteria are met.

4.4 Multi-objective hybrid improved GA-SA

Kirkpatrick et al. (1983) introduced simulated annealing as a solution to address large-scale combinatorial optimization problems.

Inputs: Sets and parameters of the problem
Outputs: Decision variables and the best non-dominated solutions
Begin:
  Step 0. (initialization)
  Generate n_{pop} (archive size) solutions randomly, apply decoding procedure and evaluate the solutions (calculate both objectives) and store them in pop
  Apply non-dominated sorting and crowding distance procedures
  Step 1. (Hybrid GA-SA main loop)
  for $it = 1$: Max-iteration
  %GA operations
    for $i = 1: n_c/2$
      Select the crossover type randomly
      Select two solutions (parents) randomly from population
      Apply crossover on the selected parents and obtain offspring
      Apply decoding procedure and evaluate the solutions and store the solutions in pop_c
    end
    Merge pop_c and pop and apply non-dominated sorting and crowding distance procedures
    store n_e number of best solutions (elites) in elites archive (pop_e)
    for $i = 1: n_m$
      Select a solution (parents) randomly from population
      Apply mutation containing local search
      Apply decoding procedure and evaluate the solutions and store the solutions in pop_m
    end
    Apply non-dominated sorting and crowding distance procedures
    for $i = 1: n_m$
      Compare the solution i of pop_m with the first solution of pop_e
      If solution i is dominated
        Replace sol_i of pop_m with sol_i^e of pop_e and remove the first solution of pop_e
        If $pop_e = []$
          Break the loop
        end
      end
    end
    Merge pop_c, pop_m and pop and apply non-dominated sorting and crowding distance procedures
    Save n_{pop} number of best solutions and remove others to update pop
    Set $T = T_0$
    for $i = 1: n_{pop}$
      Select mutation type randomly and apply it to obtain sol_i^{new}
      Calculate both objective functions for sol_i^{new}
      if $\Delta f_1 \geq 0$ && $\Delta f_2 \geq 0$ || $\Delta f_1 \leq 0$ && $\Delta f_2 \leq 0$
        Add sol_i^{new} to pop
      else if $\Delta f_1 \geq 0$ && $\Delta f_2 \leq 0$
        $sol_i = sol_i^{new}$
      else if $\Delta f_1 \leq 0$ && $\Delta f_2 \geq 0$
        if $r < \exp(\frac{-\Delta f_1}{T})$ && $r < \exp(\frac{-\Delta f_2}{T})$ (r is a random number in range [0,1])
          $sol_i = sol_i^{new}$
        end
      end
      Update temperature: $T = \alpha * T$
    end
    apply non-dominated sorting and crowding distance procedures
  end
Report best found Pareto solutions

Fig. 7. Pseudo-code of hybrid multi-objective hybrid improved GA-SA

In the proposed hybrid improved GA-SA approach, the GA operations are initially executed, followed by the implementation of simulated annealing (SA) procedures. Within the SA framework, three mutation operators are applied, namely swap, insertion, and reversion. The algorithmic procedure is depicted in Fig. 7, detailing the pseudo-code of the hybrid improved GA-SA algorithm. Within the pseudo-code, the term $\boldsymbol{\Delta f_o = f_o(x^{new}) - f_o(x^{old})}$ is employed, where x represents the solution, and $\boldsymbol{o}$ denotes the objective function.

5. Computational results and analyses

In this section, the parameters and their ranges for the problem are initially presented, derived from a real-life case application. Subsequently, the Taguchi method is employed to fine-tune the parameters of the proposed metaheuristic algorithms. The parameter settings for the model are based on this real-life case. Once the parameters for the model and solution approaches are set, the problem is solved and analyzed. The GAMS optimization software was utilized for coding the MILP model, while MATLAB was used for implementing the metaheuristics.

5.1 Case study and test problems

A real case study involving the tire SC in Iran is presented to demonstrate the practical application of the optimization model and solution approaches.

(a) Scarp tires **(b)** Tire chips

(c) Tire fiber **(d)** rubber powder

(e) Tire granulate **(f)** steel tire wire

Fig. 8. Scarp tires (a) and recycled products (b)-(f)

The tire industry, known for its recyclable products, is a growing sector with projections indicating an annual growth rate of 3.8% until 2025 (Mehrjerdi & Shafiee, 2021). Annually, millions of scrap tires are accumulated globally, posing significant environmental and health risks. These used tires can be remanufactured (retreaded) and sold in target markets at reduced prices. Additionally, various materials can be recycled from scrap tires, such as steel, rubber powder, fiber, and tire granulate, which have diverse applications. For instance, tire granulate can be used in the top asphalt layer of roads. Moreover, recycled materials like tire rubber can be repurposed for their original use, such as manufacturing new tires (Subulan et al., 2015). Fig. 8 illustrates the materials and products derived from recycling tires, respectively.

Twelve test problems were randomly generated based on the data from the case study to evaluate and compare the performance of the proposed solution methods. The dimensions of these test problems, along with those of the case study, are detailed in Table 2.

Table 2
Size of the case study and test problems

Problem No.	$\|I\|$	$\|P\|$	$\|E\|$	$\|J\|$	$\|C\|$	$\|K\|$	$\|H\|$	$\|R\|$	$\|G\|$	$\|V\|$	$\|T\|$	$\|S\|$
1	2	1	2	2	3	2	1	1	2	2	2	3
2	3	2	2	3	4	3	2	2	2	2	2	3
3	4	3	4	5	5	4	2	3	3	2	3	3
4	5	4	6	6	7	10	4	4	4	2	3	3
5	9	7	8	10	15	12	10	8	9	3	4	4
6	11	8	8	13	18	14	12	10	11	3	4	5
7	12	9	9	16	21	15	13	12	13	3	6	6
8	14	12	10	18	26	17	15	14	15	3	6	7
9	20	14	11	24	34	22	19	18	20	4	8	9
10	22	16	11	27	40	24	21	19	22	4	8	10
11	24	18	12	29	46	25	23	21	25	4	8	12
12	28	20	12	30	50	27	24	22	27	4	8	12
Case study	4	2	4	4	7	2	2	2	6	4	4	6

Table 3
Ranges of the model parameters

Parameter	Range/ Value	Parameter	Range/ Value
fs_i	[6, 12]	δ	[0.4, 0.6]
fe_{wa}	[1000, 200000]	dm_{clets}	[300, 800]
few	[150, 500]	$drclets$	[100, 300]
fcl_j	[100, 300]	drc_{glts}	[50, 200]
fcd_{ow}	[0.5, 1]	cp_i	[15000, 25000]
$tc_{ww'v}$	[0.004, 0.008]	cp_p	[5000, 10000]
distance parameters	[100, 2000] (km)	cep_p	[200, 1000]
mc_{eps}	[30, 40]	cp_j, cp_k	[12500, 25000]
ce_{pes}	[40, 50]	cl_{ow}	[1000, 5000]
hc_w	[3, 6]	cp_h	[3000, 15000]
rc_h	[0.3, 0.6]	cdp_p	[4000, 10000]
rm_{er}	[5, 10]	cp_r	[2000, 10000]
dp	[0.0004, 0.0006]	cpv_v	[5, 45]
cr_{is}	[10, 15]	$\lambda_{wats}, {\lambda'}_{pats}, \eta_{wts},$	[0, 1]
pr_{lec}	[80, 120]	φ_{vwts}	[0, 1]
${pr'}_{lec}$	[30, 60]	nv_{vwt}	[5, 20]
prc_{lg}	[2, 5]	nvt_{vt}	[20, 60]
ud_{ec}	[15, 25]	α_{ce}	[0.25, 0.95]
$\overline{ud}m_{ec}$	[8, 12]	β_e, γ_e	[0.1, 0.5]
udr_g	[1, 4]	$\tau_{cs}, \bar{\tau}_{qs}$	[0.4, 0.9]
eo_{wa}, eo_w	[1, 10]	$et_{ww'v}$	[0.0001, 0.1]
$, ep_{ep}, el_h, es_e$ em_{er}	[0.01, 0.1]		

The scenarios represent various conditions resulting from disruptions, with disruption intensities randomly generated using a uniform distribution within the intervals specified in Table 3. In all problems, the number of elements in the following sets remains constant: four capacity levels for DCs and collection centers, five price levels, and three fortification levels for all relevant facilities. The SC under consideration in the case study currently includes one factory, two DCs, and four suppliers. The company is exploring options for developing and redesigning its SC to mitigate potential disruptions and enhance network resilience. Additionally, to address environmental concerns, create a green SC, and enter new markets, the company aims to develop reverse logistics and ultimately utilize a mixed SC network. The parameter ranges for the model are provided in Table 3.

5.2 Performance metrics

Considering the multi-objective nature of the problem under study, assessing the performance of the solution methods using a simple criterion is infeasible. Therefore, this paper applies several performance metrics to measure and compare the effectiveness of the proposed multi-objective algorithms. These metrics are commonly used in literature.

- Number of Pareto Solutions (NPS): This metric indicates the number of Pareto non-dominated solutions obtained. A higher number of Pareto solutions enhances the quality and robustness of decision-making.
- Computational Time (CPU Time): This metric measures the time taken by an algorithm to obtain non-dominated solutions. Lower CPU times are preferable as they indicate more efficient algorithms.
- Quality Metric (QM): To calculate this metric, all non-dominated solutions obtained by the algorithms are stored in an archive. By comparing these solutions, the dominated ones are removed, leaving only the non-dominated solutions in the archive. The quality metric for an algorithm is the ratio of the number of its non-dominated solutions to the total number of non-dominated solutions. Higher values of this metric indicate better algorithm quality.
- Mean ideal distance (MID): MID assesses the distance of generated Pareto solutions from the ideal point, defined as the situation where the first objective is at its maximum value (f_1^{best}) and the second objective is at its minimum value (f_1^{best}). The ideal point can be considered equal to the maximum value of the first objective function and the minimum value of the second objective function among all algorithms. This metric is computed using Equation (55), where $f_{i,total}^{max}$ and $f_{i,total}^{min}$ represent the highest and lowest values of the objective functions among all obtained non-dominated solutions, respectively. n denotes the number of Pareto solutions. Lower MID values indicate higher algorithm quality (Kumar et al., 2017b)

$$MID = \frac{\sum_{i=1}^{n} \sqrt{\left(\frac{f_{1i}-f_1^{best})}{f_{1,total}^{max}-f_{1,total}^{min}}\right)^2 + \left(\frac{f_{2i}-f_2^{best})}{f_{2,total}^{max}-f_{2,total}^{min}}\right)^2}}{n} \quad (55)$$

- Spacing metric (SPM): This metric assesses the evenness of the distribution of non-dominated solutions along the Pareto frontier (Tan et al., 2006). It can be computed as follows:

$$SPM = \left[\frac{1}{n}\sum_{i=1}^{n}(d_i - \bar{d})^2\right]^{1/2} \quad (56)$$

In the aforementioned equation, d_i represents the Euclidean distance between solution i and its nearest neighbor on the Pareto frontier. The average distance, $\bar{d}$, is calculated as $\bar{d} = \sum_{i=1}^{n} d_i / n$, Where n is the number of Pareto solutions. Lower values of the Spacing Metric (SPM) are preferable as they indicate a more even distribution of solutions.

- Diversification metric (DM): This metric assesses the diversity of the non-dominated solutions identified by an algorithm. Higher DM values indicate better algorithm performance [71]. This metric can be calculated using Equation (57).

$$DM = \sqrt{(maxf_{1i} - minf_{1i})^2 + (maxf_{2i} - minf_{2i})^2} \quad (57)$$

5.3 Tuning the parameters of algorithms

In this section, the Taguchi method is employed for the tuning of metaheuristic algorithm parameters to achieve optimal performance. This approach involves the avoidance of an extensive number of experiments typically associated with full factorial experimental designs. Within the Taguchi framework, factors are categorized into controllable and noise variables, with the former influencing system performance while the latter introduces undesired variations. The concept of signal-to-noise ratio (S/N) is utilized within the Taguchi method to quantify the variation in response values. By focusing on minimizing the impact of noise factors, the robustness of the optimization process is aimed to be enhanced (Kumar et al., 2017a). Response criteria within the Taguchi method can be classified into three categories: "smaller is better," "nominal is best," and "larger is better" (Roy, 2010). For the purpose of this study, the "smaller is better" criterion is adopted for the fine-tuning of algorithm parameters.

$$S/_N = -10log\left[\frac{1}{n}\sum_{i=1}^{n} y^2\right] \quad (58)$$

Equation (58) defines y as the response value, while n represents the number of orthogonal arrays utilized in the study. The process of parameter tuning for algorithms begins by establishing the levels of parameters associated with them, as outlined in Table 4. These parameter levels, denoted by Ψ, encompass various facets including input (I), processing (P), job (J), constraints (C), kernel (K), resource (R), heuristic (H), and genetic (G) elements. The selection of these values is informed by extensive experimentation and thorough review of pertinent literature. Subsequently, a Taguchi design is constructed using Minitab software, facilitating the creation of an experimental setup. This design is then subjected to analysis to discern the most effective parameter levels, optimizing algorithm performance. The Taguchi method is employed to establish L^{27} orthogonal arrays tailored for parameter tuning within the algorithms. Fig. 9- Fig. 11 portray the signal-to-noise S/N diagrams generated as part of this process. Experimentation is conducted using test problem number 4 as the basis. Notably, the bold entries in Table 4 signify the chosen levels deemed appropriate for the study.

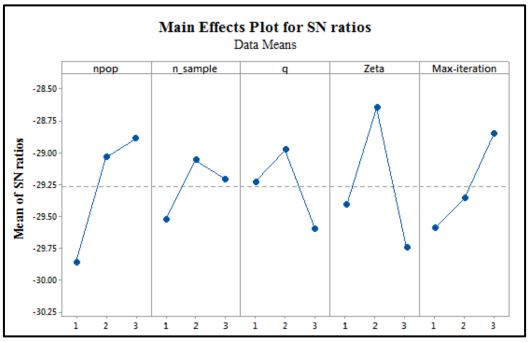

Fig. 9. Signal to noise ratio diagram for multi-objective hybrid ACO-TLBO

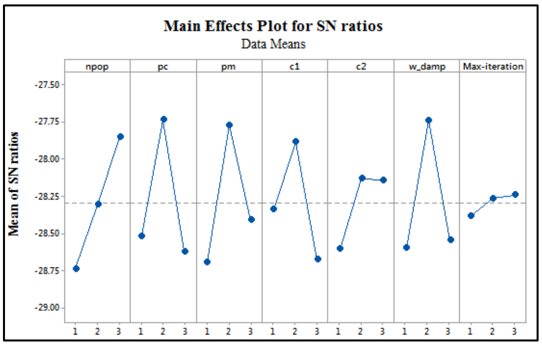

Fig. 10. Signal to noise ratio diagram for multi-objective hybrid improved GA-PSO

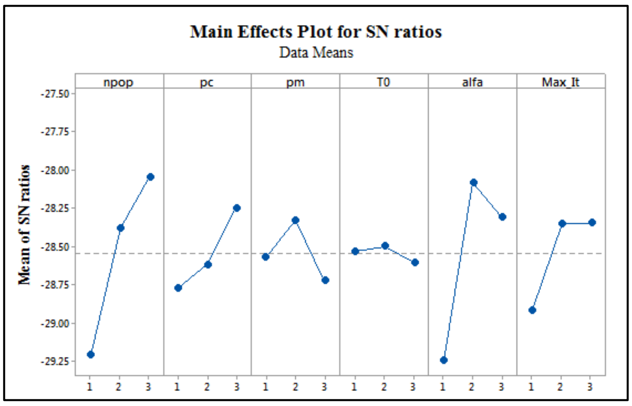

Fig. 11. Signal to noise ratio diagram for multi-objective hybrid improved GA-SA

Table 4

Parameter of the proposed algorithms and their levels

Algorithms	Parameters	Parameter Level		
		Level 1	Level 2	Level 3
ACO-TLBO	n_{pop}	50	100	**150**
	n_{sample}	10	**15**	20
	q	0.50	**1.00**	1.50
	ζ	0.50	**1.00**	1.50
	Max-iteration	$4 * \Psi$	$6 * \Psi$	$\mathbf{8 * \Psi}$
GA-PSO	n_{pop}	50	100	**150**
	p_c	0.70	**0.80**	0.90
	p_m	0.05	**0.10**	0.15
	c_1	1.50	**1.75**	2
	c_2	1.50	**1.75**	2
	w_damp	0.99	**0.95**	0.90
	Max-iteration	$4 * \Psi$	$6 * \Psi$	$\mathbf{8 * \Psi}$
GA-SA	n_{pop}	50	100	**150**
	p_c	0.50	0.70	**0.80**
	p_m	0.05	**0.10**	0.15
	T_0	30	**40**	50
	α	0.99	**0.9**	0.88
	Max-iteration	$6 * \Psi$	$\mathbf{8 * \Psi}$	$10 * \Psi$

5.4 Results and discussion

In this section, the test problems and case study are addressed using the developed solution approaches. Performance measures are employed to compare and evaluate the effectiveness of the algorithms, with the results presented in Table 5. To validate the algorithms, the augmented ε-constraint method is applied. However, this method is unable to solve medium and large-sized problems, as demonstrated by the results. The number of grid points is set to 20 (for detailed information on the augmented ε-constraint method, see Mavrotas (2009). A time limit of 60,000 seconds is established for all solution methods (NA indicates that no feasible solution was found within the specified time limit). The CPU time spent solving small-sized problems further underscores the NP-hardness of the problem.

Table 5
Evaluation of proposed solution methods based on performance metrics

Problem no.	NPS				MID			
	Aug. ε-constraint	GA-PSO	ACO-TLBO	GA-SA	Aug. ε-constraint	GA-PSO	ACO-TLBO	GA-SA
1	20	20	20	18	0.74	0.74	0.74	0.77
2	20	23	21	17	0.68	0.70	0.68	0.72
3	20	26	22	24	0.87	0.89	0.84	0.94
4	20	24	25	21	0.81	0.85	0.78	0.90
5	NA	24	21	22	NA	0.71	0.66	0.75
6	NA	28	27	28	NA	0.76	0.64	0.79
7	NA	34	30	31	NA	0.88	0.75	0.89
8	NA	30	26	28	NA	0.78	0.67	0.79
9	NA	32	28	31	NA	0.91	0.81	0.94
10	NA	36	32	35	NA	1.02	0.92	1.12
11	NA	25	19	22	NA	0.83	0.76	0.86
12	NA	31	26	30	NA	0.69	0.60	0.75
Case study	20	22	19	20	0.89	0.92	0.90	0.95
Mean (*M*i)	--	**27.31**	24.31	25.15	--	0.82	**0.75**	0.86
*M*i*		**27.31**			*M*i*		**0.75**	

Problem no.	QM				DM			
	Aug. ε-constraint	GA-PSO	ACO-TLBO	GA-SA	Aug. ε-constraint	GA-PSO	ACO-TLBO	GA-SA
1	1.00	1.00	1.00	0.90	291300.85	291300.85	291300.85	285369.12
2	0.56	0.50	0.56	0.45	375601.10	286346.56	309985.08	270005.36
3	0.47	0.27	0.41	0.20	412256.45	316413.21	322398.65	304986.77
4	0.40	0.26	0.35	0.18	482001.22	376251.12	381211.41	340365.85
5	NA	0.35	0.47	0.28	NA	621511.19	649325.82	612895.32
6	NA	0.44	0.55	0.31	NA	676252.90	690210.37	655211.23
7	NA	0.56	0.68	0.43	NA	730230.56	749510.61	710320.80
8	NA	0.45	0.61	0.35	NA	782521.64	791265.59	762941.40
9	NA	0.39	0.47	0.24	NA	1262310.85	1252303.48	1002103.25
10	NA	0.64	0.70	0.42	NA	1450362.67	1452389.01	1262300.85
11	NA	0.43	0.54	0.22	NA	1562542.06	1626402.60	1414365.70
12	NA	0.48	0.66	0.34	NA	1625321.94	1823563.12	1772003.81
Case study	0.48	0.12	0.31	0.10	259995.58	256623.41	258231.88	251438.45
Mean (*M*i)	--	0.45	**0.56**	0.34	--	787537.61	**815238.34**	741869.84
*M*i*		**0.56**				**815238.34**		

Problem no.	SPM				CPU time			
	Aug. ε-constraint	GA-PSO	ACO-TLBO	GA-SA	Aug. ε-constraint	GA-PSO	ACO-TLBO	GA-SA
1	0.39	0.39	0.39	0.38	44250.23	615.96	543.26	520.13
2	0.46	0.42	0.45	0.41	49532.65	701.32	744.23	636.99
3	0.41	0.48	0.45	0.42	54465.23	848.23	845.60	710.45
4	0.40	0.35	0.37	0.39	58128.90	1268.46	1126.31	938.16
5	NA	0.42	0.38	0.45	NA	1750.51	1690.24	1382.36
6	NA	0.47	0.51	0.45	NA	2078.65	1876.32	1801.27
7	NA	0.59	0.48	0.54	NA	2550.32	2409.95	2250.42
8	NA	0.42	0.39	0.37	NA	2968.12	2784.29	2551.45
9	NA	0.28	0.25	0.31	NA	4980.19	4513.74	4262.23
10	NA	0.56	0.41	0.48	NA	5882.13	5623.11	5320.85
11	NA	0.47	0.39	0.42	NA	6712.85	6254.12	6088.71
12	NA	0.40	0.38	0.44	NA	7652.23	7165.43	6950.65
Case study	0.49	0.69	0.40	0.36	58632.12	825.12	782.19	756.17
Mean (*M*i)	--	0.46	**0.40**	0.42	--	2987.24	2796.83	**2628.45**
*M*i*		**0.40**				**2628.45**		

To identify the most effective algorithm, the filtering/displaced ideal solution (DIS) approach is utilized (Pasandideh et al., 2015). The implementation of this method begins with the calculation of M_i values, which represent the average performance metrics for each algorithm across all problems. Next, the ideal solution (M_i^*) is determined as the best M_i value among the algorithms for each metric. Subsequently, the M_i values are normalized using the formula $M_i^N = \frac{M_i - M_i^*}{N}$, where N is the number of problems. The direct distance for each solution method is then computed using Equation (59). The algorithm with the smallest direct distance value is deemed the best. These results are presented in Table 6.

Based on the calculated direct distance values, the ACO-TLBO algorithm is identified as the superior solution method, as it has the smallest direct distance value. The Pareto fronts for the case study problem, generated by the three algorithms, are shown in Fig. 12. Fig. 13 illustrates the locations of existing and potential new facilities, along with the selected locations for the SCN in the case study.

$$\text{Direct distance}=\sum_i |M_i^N| \tag{59}$$

Table 6
Values of M_i^N and direct distance

Metrics	Algorithms		
	GA-PSO	ACO-TLBO	GA-SA
NPS	0.000	-0.110	-0.079
MID	0.095	0.000	0.146
QM	-0.194	0.000	-0.395
DM	-0.034	0.000	-0.090
SPM	0.131	0.000	0.032
CPU	0.137	0.064	0.000
Direct distance	0.591	**0.174**	0.742

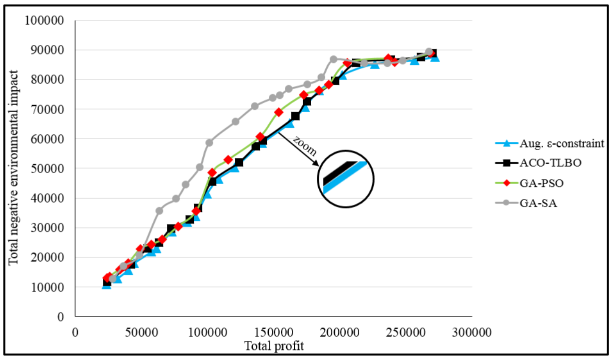

Fig.12. Pareto fronts obtained by solution methods for the problem of the case study

Fig. 13. Map of Iran and the location of facilities of the supply chain network related to the case problem

Considering the disruption risks inherent in the SC network, several resilience strategies are proposed to enhance SC resilience and manage disruptions effectively. The impacts of these resilience strategies on SC objectives are examined through a detailed analysis using the case study. Fig. 14 illustrates the influence of resilience strategies on objective functions. The analysis encompasses the following eight conditions:

- Condition 1: Only multiple sourcing is applied, with no other resilience strategies.
- Condition 2: Both multiple sourcing and facility fortification strategies are implemented.
- Condition 3: Multiple sourcing is combined with capacity expansion strategies.
- Condition 4: Dual-channel distribution strategies are applied alongside multiple sourcing.
- Condition 5: Dynamic pricing strategies are integrated with multiple sourcing.
- Condition 6: Lateral transshipment strategies are used in conjunction with multiple sourcing.
- Condition 7: Backup vehicles are employed as a strategy in addition to multiple sourcing.
- Condition 8: All proposed resilience strategies are applied simultaneously.

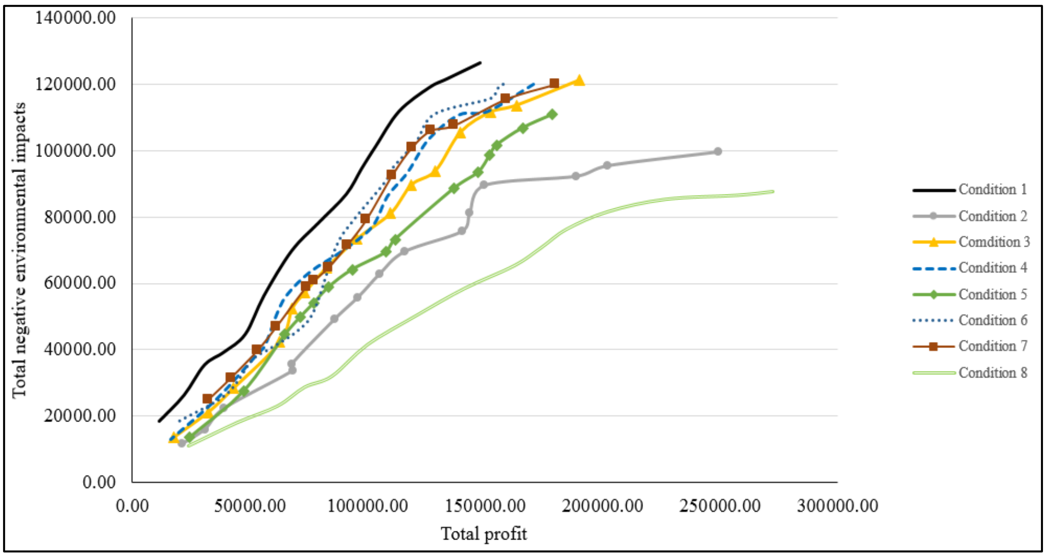

Fig. 14. investigating the effect of resilience on supply chain objectives

The Pareto fronts reveal significant impacts of resilience strategies on various objectives within the SC. Enhancing facility fortification by 46%, implementing dynamic pricing by 39%, expanding capacity by 27%, employing backup vehicles by 24%, facilitating lateral transshipment by 23%, and adopting dual-channel distribution by 17% collectively improve SC profitability compared to non-resilient conditions (Condition 8). Additionally, the integration of all strategies yields an average SC profit increase of 82%. Conversely, on the secondary objective function, bolstering facility fortification by 21%, dynamic pricing by 9%, dual-channel distribution by 6%, capacity expansion by 5%, utilizing backup vehicles by 4%, lateral transshipment by 1%, and employing all strategies concurrently result in a 28% reduction in SC negative environmental impacts. The optimization of objective functions, depicted in Fig. 15, illustrates the efficacy of resilience strategies. Specifically, Fig. 15(a) showcases the optimization of the first objective function independently, while Fig. 15(b) illustrates the same for the second objective function. These findings underscore the effectiveness of resilience strategies in addressing SC objectives.

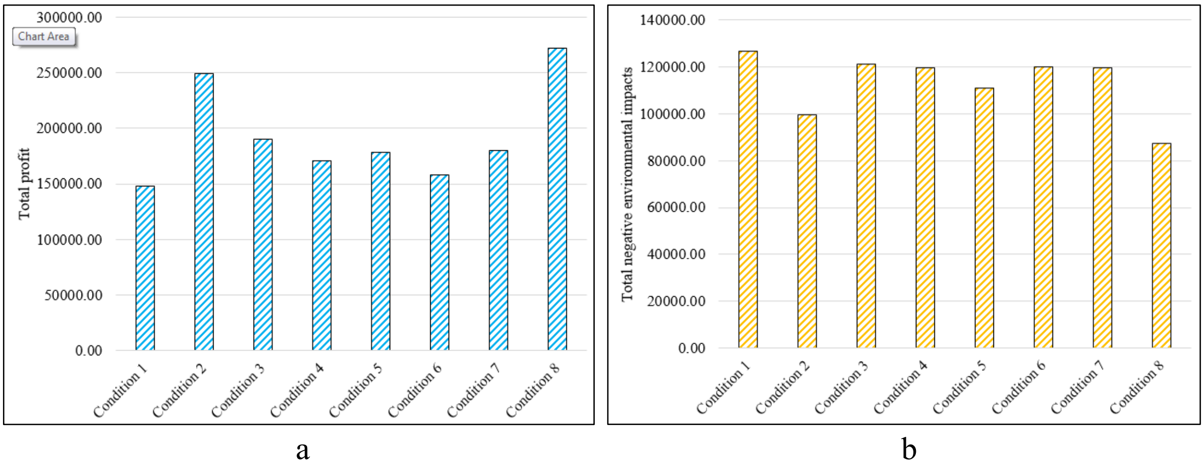

Fig. 15. Investigating the effects of resileince strategies on The first objective (a) and the second objective (b)

The depiction in Fig. 16 delineates the ramifications of SC resilience on the quantities of recycled products and materials generated, alongside the quantities of products either disposed of or released into the environment. The visual representation underscores the substantial influence of SC resilience in mitigating adverse environmental effects and preserving finite resources. Notably, within resilient SC configurations, there is a marked decrease in the volume of products disposed of or released into the environment. Conversely, there is a notable increase in the volume of recycled materials and products. Thus, the significance of SC resilience is underscored, particularly in the context of upholding environmental sustainability principles.

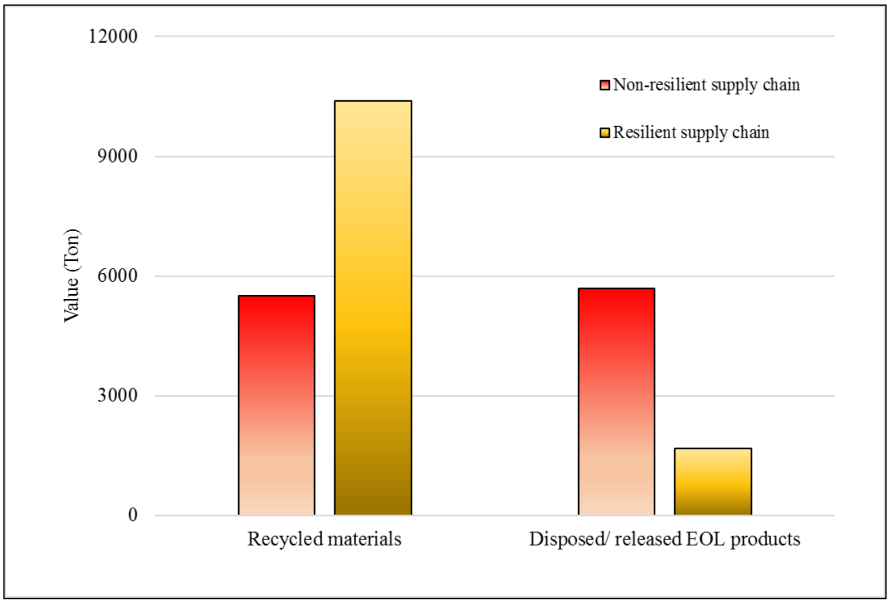

Fig. 16. Recycled materials, and released EOL products in resilient and non-resilient supply chain

In Fig. 17 and Fig. 18, a sensitivity analysis on the responsiveness rate is portrayed. These figures present the objective function values corresponding to varying responsiveness rates for main, remanufactured, and recycled products. Each figure isolates the optimization of the pertinent objective function, disregarding the influence of other objectives.

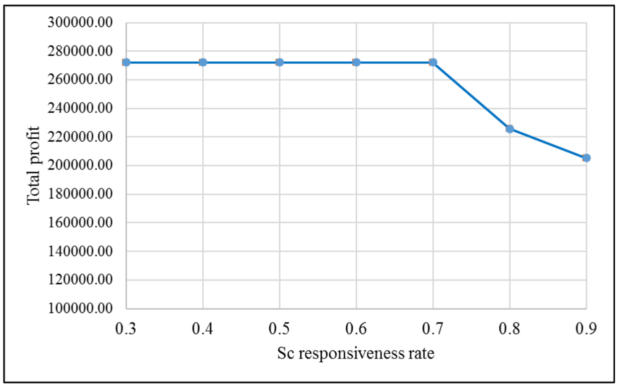

Fig. 17. Effects of changing responsiveness rates on the total cost of supply chain

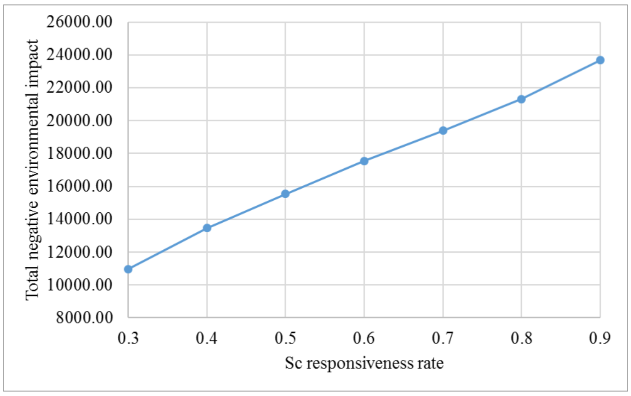

Fig. 18. Effects of changing responsiveness rates on the total negative environmental impact of supply

The results align with our expectations and appear logical. For the first objective function, which focuses on maximizing profit, the objective function remains constant within a responsiveness rate range of 0.3 to 0.7. This constancy is because the SC can meet up to approximately 70% of customer demand within this range, as dictated by the responsiveness constraints. However, as the responsiveness rate increases beyond this range, the SC struggles to meet demand, leading to higher shortage costs and subsequently reduced profitability. In relation to the second objective function, which aims to minimize negative environmental impacts, the problem inherently attempts to reduce production and other activities to lower the objective function. However, the constraints on responsiveness prevent the objective function from approaching zero. Moreover, as the responsiveness rate increases, there is a corresponding increase in production, transportation, and other activities. This escalation leads to a deterioration in the second objective function, reflecting heightened negative environmental effects.

5.5 Managerial insights

The case study examined in this research focuses on the tire industry. Nevertheless, the model presented is versatile and can be adapted for use in other industries with minimal modifications. Managers and engineers within the tire industry, as well as other sectors, can leverage insights from this study to identify disruption and operational risks within their SCs. The stochastic model and resilience strategies presented can be utilized to address these risks effectively. It is crucial to note that when disruptions impact SC facilities, companies face challenges in product production and delivery to demand zones. This inability to meet customer demands leads to increased shortage costs, reduced sales revenues, and potential financial losses for the company. Furthermore, a lack of resilience in the SCN exacerbates negative environmental impacts. As SC capacity diminishes, more new facilities need to be established to meet demand, increasing the amount of transportation required. Additionally, disruptions can halt or reduce reverse logistics activities, resulting in more waste products being released into the environment and a higher consumption of raw materials, thus amplifying the negative environmental effects. Implementing resilience strategies can help mitigate these adverse impacts. The proposed model aids industrial managers and decision-makers in various critical areas, including supplier selection, facility location determination, material and product flow management between facilities, and product pricing. Managers can utilize the Pareto fronts generated by the solution methods to select optimal points that balance economic and environmental objectives according to their company's policies and guidelines. This study serves as a valuable guide for companies aiming to withstand disruptions while maintaining their economic and environmental goals and ensuring responsiveness.

6. Conclusion

In contemporary SCs, various disruptions pose significant threats to their survival and efficiency. These disruptions can adversely affect the environmental and economic objectives that are critical to stakeholders. Consequently, ensuring SC resilience is crucial to safeguarding these objectives. This study investigates the SCND problem with a focus on resilience and environmental sustainability. The examined SC network incorporates both open and closed-loop structures while accounting for operational and disruption risks. To address disruptions, several resilience strategies were implemented, and the problem's uncertainty was managed through a scenario-based two-stage stochastic programming approach. Given the complexity of the problem, a novel hybrid metaheuristic called ACO-TLBO was developed. Additionally, two other hybrid metaheuristics—hybrid improved GA-PSO and hybrid improved GA-SA—were formulated to solve the problem and compare solution methodologies. The augmented ε-constraint method was employed to validate the algorithms. The metaheuristics' parameters were fine-tuned using the Taguchi method, and comparative analyses were conducted using various test problems. According to the filtering/displaced ideal solution method results, the ACO-TLBO algorithm emerged as the most effective. A real-life case study was conducted to further analyze and demonstrate the applicability and validity of the proposed model and solution methods. The results indicated that the introduced resilience strategies significantly enhance both economic and environmental objectives compared to non-resilient approaches. Analyses based on eight different conditions revealed that applying all proposed resilience strategies could increase SC profit by 82% and reduce negative environmental impacts by 28%. The findings underscore the necessity of integrating resilience considerations with environmental aspects. A sensitivity analysis on the responsiveness rate confirmed the model's accuracy and highlighted the importance of this parameter. The mathematical model, solution methods, and results presented in this study are valuable for managers and engineers involved in SCM.

Future research could extend the field of resilient SC network design (SCND) by integrating the developed model with other problems, such as the vehicle routing problem. Additionally, future studies might explore the development of exact solution methods or other metaheuristics for solving the proposed model. Investigating other types of uncertainties, such as deep and epistemic uncertainties, also presents an intriguing avenue for researchers aiming to optimize SC networks under uncertainty.

Acknowledgment

The authors acknowledge that an earlier version of this manuscript was made available as a preprint on Research Square (DOI: https://doi.org/10.21203/rs.3.rs-1140812/v1).

References

Abbasian, M., Sazvar, Z., & Mohammadisiahroudi, M. (2023). A hybrid optimization method to design a sustainable resilient supply chain in a perishable food industry. *Environmental science and pollution research*, *30*(3), 6080-6103.

Arabi, M., & Gholamian, M. R. (2023). Resilient closed-loop supply chain network design considering quality uncertainty: A case study of stone quarries. *Resources Policy*, *80*, 103290.

Azad, N., Saharidis, G. K., Davoudpour, H., Malekly, H., & Yektamaram, S. A. (2013). Strategies for protecting supply chain networks against facility and transportation disruptions: an improved Benders decomposition approach. *Annals of Operations Research*, *210*(1), 125-163.

Boronoos, M., Mousazadeh, M., & Torabi, S. A. (2021). A robust mixed flexible-possibilistic programming approach for multi-objective closed-loop green supply chain network design. *Environment, Development and Sustainability*, *23*(3), 3368-3395.

Bottani, E., Murino, T., Schiavo, M., & Akkerman, R. (2019). Resilient food supply chain design: Modelling framework and metaheuristic solution approach. *Computers & Industrial Engineering*, *135*, 177-198.

Deb, K., Pratap, A., Agarwal, S., & Meyarivan, T. (2002). A fast and elitist multiobjective genetic algorithm: NSGA-II. *IEEE transactions on evolutionary computation*, *6*(2), 182-197.

Dehshiri, S. J. H., & Amiri, M. (2024). Considering the circular economy for designing closed-loop supply chain under hybrid uncertainty: A robust scenario-based possibilistic-stochastic programming. *Expert Systems with Applications*, *238*, 121745.

Dorigo, M. (1992). Optimization, learning and natural algorithms. *Ph. D. Thesis, Politecnico di Milano*.

Dorigo, M., Di Caro, G., & Gambardella, L. M. (1999). Ant algorithms for discrete optimization. *Artificial life*, *5*(2), 137-172.

Dorigo, M., Maniezzo, V., & Colorni, A. (1996). Ant system: optimization by a colony of cooperating agents. *IEEE Transactions on Systems, Man, and Cybernetics, Part B (Cybernetics)*, *26*(1), 29-41.

Fahimnia, B., Jabbarzadeh, A., & Sarkis, J. (2018). Greening versus resilience: A supply chain design perspective. *Transportation Research Part E: Logistics and Transportation Review*, *119*, 129-148.

Fattahi, M., Govindan, K., & Keyvanshokooh, E. (2017). Responsive and resilient supply chain network design under operational and disruption risks with delivery lead-time sensitive customers. *Transportation Research Part E: Logistics and Transportation Review*, *101*, 176-200.

Fattahi, M., Govindan, K., & Keyvanshokooh, E. (2018). A multi-stage stochastic program for supply chain network redesign problem with price-dependent uncertain demands. *Computers & Operations Research*, *100*, 314-332.

Fazli-Khalaf, M., Naderi, B., Mohammadi, M., & Pishvaee, M. S. (2021). The design of a resilient and sustainable maximal covering closed-loop supply chain network under hybrid uncertainties: a case study in tire industry. *Environment, Development and Sustainability*, *23*(7), 9949-9973.

Feitó-Cespón, M., Costa, Y., Pishvaee, M. S., & Cespón-Castro, R. (2021). A fuzzy inference based scenario building in two-stage optimization framework for sustainable recycling supply chain redesign. *Expert Systems with Applications*, *165*, 113906.

Feitó-Cespón, M., Sarache, W., Piedra-Jimenez, F., & Cespón-Castro, R. (2017). Redesign of a sustainable reverse supply chain under uncertainty: A case study. *Journal of cleaner production*, *151*, 206-217.

Gen, M., Altiparmak, F., & Lin, L. (2006). A genetic algorithm for two-stage transportation problem using priority-based encoding. *OR spectrum*, *28*(3), 337-354.

Ghavamifar, A., Makui, A., & Taleizadeh, A. A. (2018). Designing a resilient competitive supply chain network under disruption risks: A real-world application. *Transportation Research Part E: Logistics and Transportation Review*, *115*, 87-109.

Gholami-Zanjani, S. M., Jabalameli, M. S., & Pishvaee, M. S. (2021). A resilient-green model for multi-echelon meat supply chain planning. *Computers & Industrial Engineering*, *152*, 107018.

Ghomi-Avili, M., Naeini, S. G. J., Tavakkoli-Moghaddam, R., & Jabbarzadeh, A. (2018). A fuzzy pricing model for a green competitive closed-loop supply chain network design in the presence of disruptions. *Journal of Cleaner Production*, *188*, 425-442.

Govindan, K., Fattahi, M., & Keyvanshokooh, E. (2017). Supply chain network design under uncertainty: A comprehensive review and future research directions. *European journal of operational research*, *263*(1), 108-141.

Govindan, K., Paam, P., & Abtahi, A.-R. (2016). A fuzzy multi-objective optimization model for sustainable reverse logistics network design. *Ecological indicators*, *67*, 753-768.

Hasani, A., & Khosrojerdi, A. (2016). Robust global supply chain network design under disruption and uncertainty considering resilience strategies: A parallel memetic algorithm for a real-life case study. *Transportation Research Part E: Logistics and Transportation Review*, *87*, 20-52.

Hasani, A., Mokhtari, H., & Fattahi, M. (2021). A multi-objective optimization approach for green and resilient supply chain network design: a real-life case study. *Journal of Cleaner Production*, *278*, 123199.

Holland, J. H. (1975). Adaption in natural and adaptive systems. In: University of Michigan Press, Ann Arbor.

Hosseini, S., Ivanov, D., & Dolgui, A. (2019). Review of quantitative methods for supply chain resilience analysis. *Transportation Research Part E: Logistics and Transportation Review*, *125*, 285-307.

Ivanov, D., & Dolgui, A. (2020). Viability of intertwined supply networks: extending the supply chain resilience angles towards survivability. A position paper motivated by COVID-19 outbreak. *International Journal of Production Research*, *58*(10), 2904-2915.

Jabbarzadeh, A., Fahimnia, B., & Sabouhi, F. (2018). Resilient and sustainable supply chain design: sustainability analysis under disruption risks. *International Journal of Production Research*, *56*(17), 5945-5968.

Jabbarzadeh, A., Fahimnia, B., Sheu, J.-B., & Moghadam, H. S. (2016). Designing a supply chain resilient to major disruptions and supply/demand interruptions. *Transportation Research Part B: Methodological*, *94*, 121-149.

Jabbarzadeh, A., Haughton, M., & Khosrojerdi, A. (2018). Closed-loop supply chain network design under disruption risks: A robust approach with real world application. *Computers & industrial engineering*, *116*, 178-191.

Karmaker, C. L., Ahmed, T., Ahmed, S., Ali, S. M., Moktadir, M. A., & Kabir, G. (2021). Improving supply chain sustainability in the context of COVID-19 pandemic in an emerging economy: Exploring drivers using an integrated model. *Sustainable production and consumption*, *26*, 411-427.

Kennedy, J., & Eberhart, R. (1995). Particle swarm optimization. Proceedings of ICNN'95-international conference on neural networks,

Kirkpatrick, S., Gelatt, C. D., & Vecchi, M. P. (1983). Optimization by Simulated Annealing. *Science*, *220*(4598), 671-680. https://doi.org/doi:10.1126/science.220.4598.671

Klibi, W., Martel, A., & Guitouni, A. (2010). The design of robust value-creating supply chain networks: a critical review. *European Journal of Operational Research*, *203*(2), 283-293.

Kumar, P., Herbert, M., & Rao, S. (2017a). Population based metaheuristic algorithm approach for analysis of multi-item multi-period procurement lot sizing problem. *Advances in Operations Research*, *2017*.

Kumar, P., Herbert, M., & Rao, S. (2017b). Population Based Metaheuristic Algorithm Approach for Analysis of Multi-Item Multi-Period Procurement Lot Sizing Problem. *Advances in Operations Research*, *2017*, 1-18. https://EconPapers.repec.org/RePEc:hin:jnlaor:3601217

Li, Z., & Zhang, C. (2024). Designing a two-stage model for the resilient agri-food supply chain network under dynamic competition. *British Food Journal*, *126*(2), 662-681.

Liao, T., Socha, K., de Oca, M. A. M., Stützle, T., & Dorigo, M. (2013). Ant colony optimization for mixed-variable optimization problems. *IEEE transactions on evolutionary computation*, *18*(4), 503-518.

Mardan, E., Govindan, K., Mina, H., & Gholami-Zanjani, S. M. (2019). An accelerated benders decomposition algorithm for a bi-objective green closed loop supply chain network design problem. *Journal of Cleaner Production*, *235*, 1499-1514.

Mavrotas, G. (2009). Effective implementation of the ε-constraint method in multi-objective mathematical programming problems. *Applied mathematics and computation*, *213*(2), 455-465.

Mehrjerdi, Y. Z., & Shafiee, M. (2021). A resilient and sustainable closed-loop supply chain using multiple sourcing and information sharing strategies. *Journal of cleaner production*, *289*, 125141.

Meng, J., Hu, X., Chen, P., Coffman, D. M., & Han, M. (2020). The unequal contribution to global energy consumption along the supply chain. *Journal of environmental management*, *268*, 110701.

Michalewicz, Z., Vignaux, G. A., & Hobbs, M. (1991). A nonstandard genetic algorithm for the nonlinear transportation problem. *ORSA Journal on computing*, *3*(4), 307-316.

Mohammed, A., Harris, I., Soroka, A., & Nujoom, R. (2019). A hybrid MCDM-fuzzy multi-objective programming approach for a G-resilient supply chain network design. *Computers & Industrial Engineering*, *127*, 297-312.

Mohtashami, Z., Aghsami, A., & Jolai, F. (2020). A green closed loop supply chain design using queuing system for reducing environmental impact and energy consumption. *Journal of cleaner production*, *242*, 118452.

Moncayo-Martínez, L. A., & Zhang, D. Z. (2011). Multi-objective ant colony optimisation: A meta-heuristic approach to supply chain design. *International Journal of Production Economics*, *131*(1), 407-420.

Namdar, J., Li, X., Sawhney, R., & Pradhan, N. (2018). Supply chain resilience for single and multiple sourcing in the presence of disruption risks. *International Journal of Production Research*, *56*(6), 2339-2360.

Nikian, A., Khademi Zare, H., Lotfi, M. M., & Fallah Nezhad, M. S. (2023). Redesign of a sustainable and resilient closed-loop supply chain network under uncertainty and disruption caused by sanctions and COVID-19. *Operations Management Research*, *16*(2), 1019-1042.

Nurjanni, K. P., Carvalho, M. S., & Costa, L. (2017). Green supply chain design: A mathematical modeling approach based on a multi-objective optimization model. *International Journal of Production Economics*, *183*, 421-432.

Pasandideh, S. H. R., Niaki, S. T. A., & Asadi, K. (2015). Optimizing a bi-objective multi-product multi-period three echelon supply chain network with warehouse reliability. Expert Systems with Applications, 42(5), 2615-2623.

Peng, P., Snyder, L. V., Lim, A., & Liu, Z. (2011). Reliable logistics networks design with facility disruptions. *Transportation Research Part B: Methodological*, *45*(8), 1190-1211.

Rad, R. S., & Nahavandi, N. (2018). A novel multi-objective optimization model for integrated problem of green closed loop supply chain network design and quantity discount. *Journal of cleaner production*, *196*, 1549-1565.

Rajesh, R. (2020). Network design for resilience in supply chains using novel crazy elitist TLBO. *Neural Computing and Applications*, *32*(11), 7421-7437.

Ramezanian, R., Vali-Siar, M. M., & Jalalian, M. (2019). Green permutation flowshop scheduling problem with sequence-dependent setup times: a case study. *International Journal of Production Research*, *57*(10), 3311-3333.

Rao, R. V., Savsani, V. J., & Vakharia, D. P. (2011). Teaching–learning-based optimization: a novel method for constrained mechanical design optimization problems. *Computer-aided design*, *43*(3), 303-315.

Rezaei, A., & Liu, Q. (2024). A multi objective optimization framework for robust and resilient supply chain network design using NSGAII and MOPSO algorithms. International Journal of Industrial Engineering Computations, 15(3), 773-790.

Rezapour, S., Farahani, R. Z., & Pourakbar, M. (2017). Resilient supply chain network design under competition: a case study. *European Journal of Operational Research*, *259*(3), 1017-1035.

Ribeiro, J. P., & Barbosa-Póvoa, A. P. F. (2023). A responsiveness metric for the design and planning of resilient supply chains. *Annals of operations research*, *324*(1), 1129-1181.

Roy, R. K. (2010). *A primer on Taguchi method* (2 ed.). society of Manufacturing Engineers.

Sabouhi, F., Jabalameli, M. S., & Jabbarzadeh, A. (2021). An optimization approach for sustainable and resilient supply chain design with regional considerations. *Computers & Industrial Engineering*, *159*, 107510.

Sabouhi, F., Jabalameli, M. S., Jabbarzadeh, A., & Fahimnia, B. (2020). A multi-cut L-shaped method for resilient and responsive supply chain network design. *International Journal of Production Research*, *58*(24), 7353-7381.

Sabouhi, F., Pishvaee, M. S., & Jabalameli, M. S. (2018). Resilient supply chain design under operational and disruption risks considering quantity discount: A case study of pharmaceutical supply chain. *Computers & industrial engineering*, *126*, 657-672.

Sadghiani, N. S., Torabi, S., & Sahebjamnia, N. (2015). Retail supply chain network design under operational and disruption risks. *Transportation Research Part E: Logistics and Transportation Review*, *75*, 95-114.
Saeed, A., Jian, M., Imran, M., & Freen, G. (2024). Green-resilient model for smartphone closed-loop supply chain network design: A novel four-valued refined neutrosophic optimization. *Computers & industrial engineering*, *190*, 110087.
Salema, M. I. G., Barbosa-Povoa, A. P., & Novais, A. Q. (2007). An optimization model for the design of a capacitated multi-product reverse logistics network with uncertainty. *European journal of operational research*, *179*(3), 1063-1077.
Sazvar, Z., Tafakkori, K., Oladzad, N., & Nayeri, S. (2021). A capacity planning approach for sustainable-resilient supply chain network design under uncertainty: A case study of vaccine supply chain. *Computers & Industrial Engineering*, *159*, 107406.
Shahparvari, S., Soleimani, H., Govindan, K., Bodaghi, B., Fard, M. T., & Jafari, H. (2021). Closing the loop: Redesigning sustainable reverse logistics network in uncertain supply chains. *Computers & industrial engineering*, *157*, 107093.
Sharma, M., Antony, R., & Tsagarakis, K. (2023). Green, resilient, agile, and sustainable fresh food supply chain enablers: Evidence from India. *Annals of operations research*, 1-27.
Shekarabi, H., Vali-Siar, M. M., & Mozdgir, A. (2024). Food supply chain network design under uncertainty and pandemic disruption. *Operational Research*, *24*(2), 26.
Socha, K., & Dorigo, M. (2008). Ant colony optimization for continuous domains. *European journal of operational research*, *185*(3), 1155-1173.
Soleimani, H., Govindan, K., Saghafi, H., & Jafari, H. (2017). Fuzzy multi-objective sustainable and green closed-loop supply chain network design. *Computers & industrial engineering*, *109*, 191-203.
Soleimani, H., & Kannan, G. (2015). A hybrid particle swarm optimization and genetic algorithm for closed-loop supply chain network design in large-scale networks. *Applied mathematical modelling*, *39*(14), 3990-4012.
Subulan, K., Taşan, A. S., & Baykasoğlu, A. (2015). Designing an environmentally conscious tire closed-loop supply chain network with multiple recovery options using interactive fuzzy goal programming. *Applied mathematical modelling*, *39*(9), 2661-2702.
Tan, K. C., Goh, C. K., Yang, Y., & Lee, T. H. (2006). Evolving better population distribution and exploration in evolutionary multi-objective optimization. *European journal of operational research*, *171*(2), 463-495.
Torabi, S., Namdar, J., Hatefi, S., & Jolai, F. (2016). An enhanced possibilistic programming approach for reliable closed-loop supply chain network design. *International Journal of Production Research*, *54*(5), 1358-1387.
Vali-Siar, M. M., & Roghanian, E. (2020). Resilient mixed supply chain network redesign under operational and disruption risks: A case study. *Journal of Industrial Engineering Research in Production Systems*, *8*(16), 113-135.
Vali-Siar, M. M., & Roghanian, E. (2022). Sustainable, resilient and responsive mixed supply chain network design under hybrid uncertainty with considering COVID-19 pandemic disruption. *Sustainable Production and Consumption*, *30*, 278-300.
Valizadeh, J., Ghahroudi, A. G., Soltani, S., Akhavan, M., Zaki, A., & Heravi, P. (2024). Mathematical modeling for the closed-loop supply chain with consideration of sustainability risks: a hybrid optimization approach. *Environment, Development and Sustainability*, 1-36.
Van Engeland, J., Beliën, J., De Boeck, L., & De Jaeger, S. (2020). Literature review: Strategic network optimization models in waste reverse supply chains. *Omega*, *91*, 102012.
Yavari, M., & Zaker, H. (2019). An integrated two-layer network model for designing a resilient green-closed loop supply chain of perishable products under disruption. *Journal of Cleaner Production*, *230*, 198-218.
Yousefi-Babadi, A., Bozorgi-Amiri, A., & Tavakkoli-Moghaddam, R. (2022). Redesigning a supply chain network with system disruption using Lagrangian relaxation: A real case study. *Soft Computing*, *26*(19), 10275-10299.
Yousefi-Babadi, A., Bozorgi-Amiri, A., Tavakkoli-Moghaddam, R., & Govindan, K. (2023). Redesign of the sustainable wheat-flour-bread supply chain network under uncertainty: An improved robust optimization. *Transportation Research Part E: Logistics and Transportation Review*, *176*, 103215.
Zhen, L., Huang, L., & Wang, W. (2019). Green and sustainable closed-loop supply chain network design under uncertainty. *Journal of Cleaner Production*, *227*, 1195-1209.
Zohal, M., & Soleimani, H. (2016). Developing an ant colony approach for green closed-loop supply chain network design: a case study in gold industry. *Journal of Cleaner Production*, *133*, 314-337.